Charles University

Faculty of Medicine in Hradec Králové

Doctoral degree programme

Medical Biology

Analysis of growth-inhibitory mechanisms of flubendazole in malignant melanoma cells

Analýza růstově inhibičních mechanismů flubendazolu u buněk maligního melanomu

PharmDr. Kristýna Čáňová

Supervisor: prof. PharmDr. Emil Rudolf, Ph.D.

Hradec Králové, 2018

DECLARATION

I declare hereby that this dissertation thesis is my own original work, and that I indicated by references all used information sources. I also agree with depositing my dissertation in the Medical Library of the Charles University, Faculty of Medicine in Hradec Králové and with making use of it for study and educational purpose provided that anyone who will use it for his/her publication or lectures is obliged to refer to or cite my work properly.

I give my consent to availability of my dissertation´s electronic version in the information system of the Charles University.

Hull, United Kingdom, 2018 Signature of the author

ACKNOWLEDGEMENTS

I would like to express my sincere gratitude to my supervisor prof. PharmDr. Emil Rudolf, Ph.D. for his support of my Ph.D. study and related research and extend my further thanks for his valuable advice and comments.

A special thanks to PharmDr. Doris Vokurková, Ph.D. who performed the analysis of cell cycle presented in this thesis and to Lucie Rozkydalová who helped me with Western blot methodology.

I would like to thank also all my colleagues at the department of Medical Biology and Genetics for their help, support and friendly atmosphere in the laboratory.

Finally, I would like to express my sincere gratitude to my family, friends, and especially to my boyfriend for their support, patience and never-ending optimism.

TABLE OF CONTENTS

1. SUMMARY (ENG)

Malignant skin melanoma is at its advanced stage highly aggressive and chemoresistant to almost all currently available therapies. Moderns efforts are thus aimed to identify new targets in melanoma cells or to take advantage of novel indications of already approved drugs – a process called drug repurposing. This work was focused on evaluation of cell growth inhibitory properties of one such drug – flubendazole (FLU) – a widely used anthelmintic compound belonging to benzimidazole family. This drug specifically interacts with β-tubulin, which results in disruption of microtubule structure and function in the exposed cells. Several members of the benzimidazole family (including FLU) have already shown the growth inhibitory potential in tumor cells derived from breast, colon, blood and nervous system malignancies. Still, the specific activity of FLU in malignant melanoma has not been tested to the date.

Cytotoxicity of FLU was tested in three malignant melanoma cell lines representing diverse melanoma molecular types (A-375, BOWES and RPMI-7951) during up to 72 hours using WST-1 and x-CELLigence assays. Based on achieved IC_{50} from individual cell lines, the 1 μM FLU concentration was selected for further testing. While relatively tolerated in normal human skin melanocytes, FLU at this concentration disrupted microtubular cytoskeleton, induced G2/M cell cycle arrest and changed morphology of exposed melanoma cells. The presence of other specific changes (i.e. cell enlargement and multinucleation, overexpression of p21 and activation of caspase-2) indicated mitotic catastrophe which was followed by apoptotic cell death. Further analyses revealed that both processes were not linked by activated TP53-BAX axis and their further elucidation should be addressed in future.

FLU activity was also evaluated in melanoma cells derived from melanoma explant cultures obtained from human subjects undergoing melanoma excision in Faculty teaching hospital in Hradec Králové. In a pilot study using cells from one patient FLU showed cytotoxicity and growth inhibitory properties, however, with lesser potency as judged from higher IC_{50} value. 1 μM FLU concentration then had cytostatic effect in exposed cells and induced a series of very unusual morphological alterations entirely dissimilar of mitotic catastrophe and classical apoptosis.

2. SUMMARY (CZE)

Maligní kožní melanom je ve svém pokročilém stádiu vysoce agresivním nádorovým onemocněním často chemorezistentním na většinu současných terapeutických strategií. V současné době se výzkumy zaměřují na identifikaci nových cílů v maligních melanocytech či se snaží využít tzv. nových indikací již schválených léčiv, a to prostřednictvím přístupů nazývaných „drug repurposing“. Tato práce se zabývá ověřováním růstově inhibičních vlastností jednoho takového léčiva – flubendazolu (FLU) – široce využívaného anthelmintika patřícího do rodiny benzimidazolových derivátů. Toto léčivo specificky interaguje s β-tubulinem, což následně vede k poškození struktury a funkce mikrotubulů v ovlivněných buňkách. Několik členů benzimidazolové rodiny (včetně FLU) již prokázalo růstově-inhibiční potenciál u nádorových buněk odvozených z nádorů prsu, tlustého střeva, krve a nervového systému. Protinádorové vlastnosti FLU u maligního melanomu však ještě do této doby nebyly ověřovány.

Cytotoxicita FLU byla testována u tří linií lidského maligního melanomu představující odlišné molekulární subtypy (A-375, BOWES a RPMI-7951) během 72 hodin pomocí WST-1 a x-CELLigence testů. Na základě jednotlivých hodnot IC_{50} získaných z jednotlivých buněčných linií byla pro další testování vybrána koncentrace FLU 1 µM. Tato koncentrace byla relativně tolerována u normálních lidských kožních melanocytů (HEM), nicméně u melanomových buněk významně poškodila organizaci a funkci mikrotubulů, indukovala zástavu buněčného cyklu v G2/M fázi a vyvolala sérii změn v buněčné morfologii. Přítomnost dalších specifických změn (tzn. vznik obrovských mnohojaderných buněk, zvýšená exprese p21 a aktivace kaspázy-2) naznačila mitotickou katastrofu, po které následovala na kaspáze-3/7 závislá apoptotická buněčná smrt. Další analýzy prokázaly, že oba procesy nespojuje aktivovaná signální dráha TP53-BAX, a jejich podrobnější mechanizmy budou tedy předmětem budoucích studií.

Protinádorová aktivita FLU byla také ověřována u melanomových buněk odvozených z explantátových kultur získaných ze vzorků melanomu od pacientů léčených ve Fakultní nemocnici Hradec Králové. V pilotní studii prováděné na buňkách vzorku od vybraného pacienta FLU vyvolal inhibici růstu a cytotoxicitu, nicméně buňky na něj vykazovaly nižší citlivost (dle získané hodnoty IC_{50}). Dále testovaná koncentrace FLU 1 µM vykazovala cytostatický účinek a vyvolávala velmi ojedinělé morfologické

změny u exponovaných buněk, významně odlišné od dříve pozorované mitotické katastrofy a apoptózy u buněk melanomových linií.

3. USED ABBREVIATIONS

ABC	ATP binding cassette
AIF	apoptosis inducing factor
ALM	acral lentiginous melanoma
APAF1	apoptotic protease activating factor 1
ATG4B	autophagy-related protein 4B
BAX	BCL2-associated X protein
BCA	bicinchoninic acid
BRAF	v-Raf murine sarcoma viral oncogene homolog B
BSA	bovine serum albumin
CDK4	cyclin-dependent kinase 4
CDKN1A	cyclin-dependent kinase inhibitor 1A
CDKN2A	cyclin-dependent kinase inhibitor 2A
CHAPS	3-[(3-cholamidopropyl)dimethylam-monio]-1-propanesulfonate hydrate
c-MYC	Myc proto-oncogene protein
CTLA-4	anti-cytotoxic T-lymphocyte antigen 4
DAPI	4',6-diamidino-2-phenylindole
DMEM	Dulbecco’s modified Eagle medium
DMSO	dimethylsulfoxide
DOPA	dihydroxyphenylalanine
DTIC	dacarbazine
DTT	dithiotreitol

EDTA	ethylenediaminetetraacetic acid
EdU	5-ethynyl-2′-deoxyuridine
EMEM	Eagle’s minimal essential medium
EMT	epithelial-to-mesenchymal transition
FBS	fetal bovine serum
FLU	flubendazole
GNA11	G Protein Subunit Alpha 11
GNAQ	guanine nucleotide-binding protein G(q) subunit alpha
HEPES	4-(2-hydroxyethyl)-1-piperazineethanesulfonic acid
IFN- α	interferon- α
IL-2	interleukin-2
LM	lentigo melanoma
MAPK	mitogen activated protein kinase
MART-1	melanoma-associated antigen recognized by T cells-1
MC1R	melanocortin 1 receptor
MDR	multi-drug resistance
MITF	microphthalmia-associated transcription factor
NM	nodular melanoma
NRAS	neuroblastoma RAS Viral Oncogene Homolog
PBS	phosphate-buffered saline
PI3K	phosphatidylinositol-3-kinise
PKC	protein kinase C
POMC	proopiomelanocortin

PTEN	phosphatase and tensin homolog
ROS	reactive oxygen species
RPM	revolutions per minute
RT	room temperature
SSM	superficial spreading melanoma
TP53	tumor protein p53
TRP1	tyrosinase-related protein 1
TRP2	tyrosinase-related protein 2
TYR	tyrosinase
WNT	Wingless-related integration site
WST	4-[3-(4-iodophenyl)-2-(4-nitrophenyl)-2H-5-tetrazolio]-1,3-benzene disulphonate
XIAP	X-linked inhibitor of apoptosis
α-MSH	α-melanocyte-stimulating hormone

4. THEORETICAL PART

4.1. Malignant melanoma

4.1.1. Definition

Melanoma is a malignant tumor arising from melanocytic cells and primarily involves the skin. The neuroectodermal origin of melanocytes explains the occurrence of tumors in other tissues too. In fact, melanomas can also arise in the eye (uvea, conjunctiva and ciliary body), meninges and on various mucosal surfaces but their occurrence is rare. Melanomas are usually heavily pigmented but they can be also amelanotic. Melanoma is characterized by aggressive growth and even small tumors may have a tendency to metastasize **(1)**.

4.1.2. Epidemiology

The incidence of cutaneous malignant melanoma is increasing worldwide in white populations, in particular in regions with excessive sun exposure of fair-skinned individuals (Figure 1).

People with light complexions, an inability to tan, blond or red hair, or blue eyes have a higher risk of melanoma than the general population. The highest incidence rates have been reported from Australia with 56 new cases per year per 100,000 for men and 43 for women **(2, 3)**.

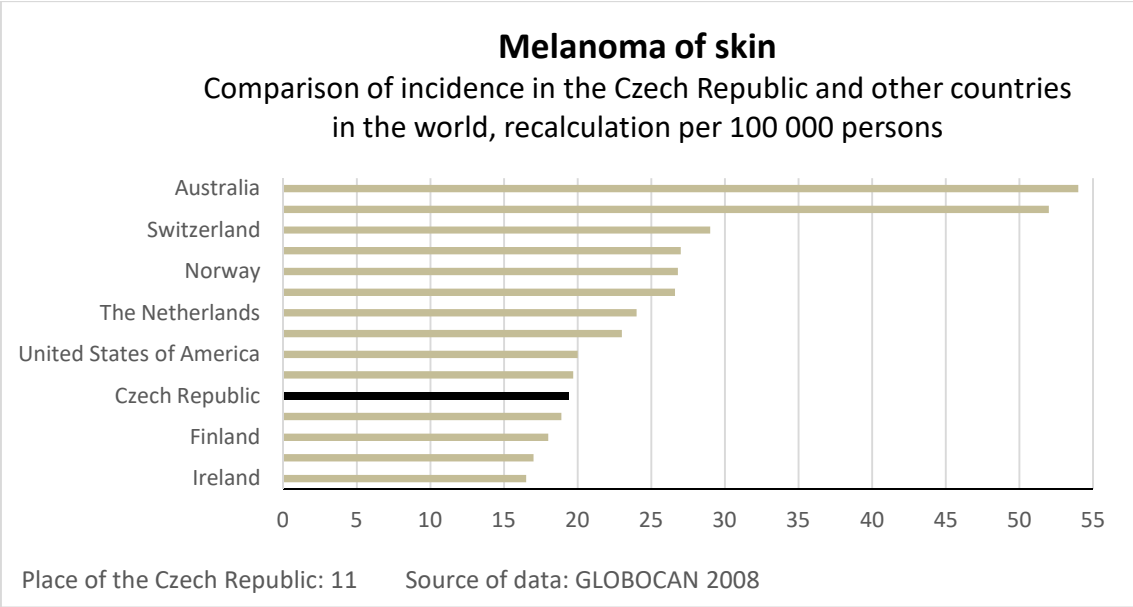

Figure 1 - Incidence of melanoma of skin in the Czech Republic and other world countries (www.svod.cz, adapted)

During the past 30 years, the incidence of melanoma of skin in the Czech Republic increased almost 5 times with reported 25.9 new cases per 100,000 inhabitants in 2012 (**4**,**5**; Figure 2).

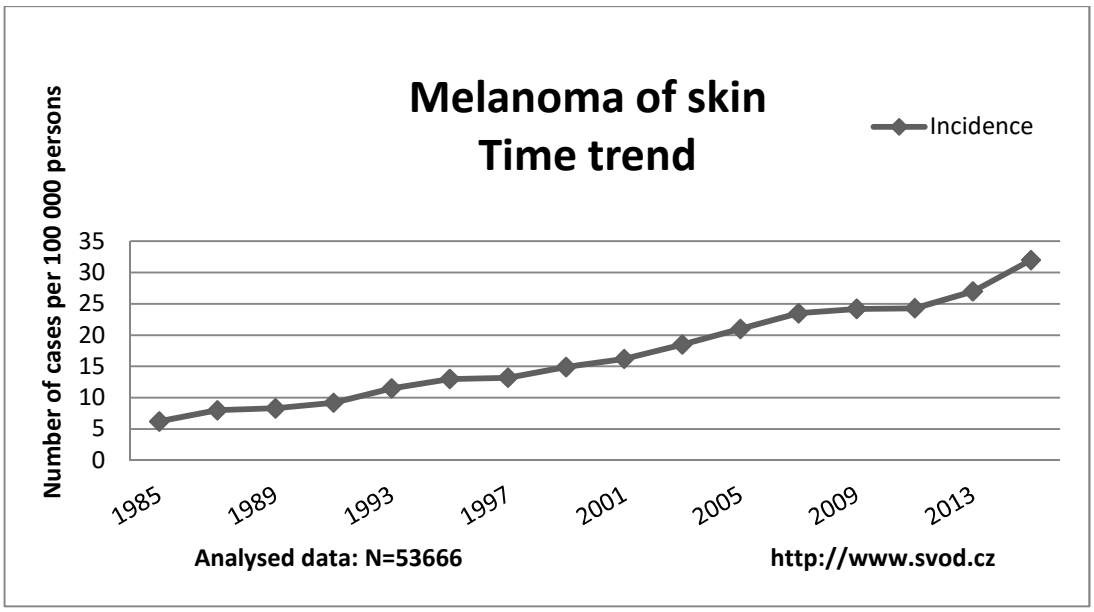

Figure 2 - Incidence of melanoma of skin in the Czech Republic (www.svod.cz, adapted)

Genetic factors play a dominant role in risk for melanoma. In addition to skin pigmentation, other heritable risk factors include family history of melanoma, density and type of existing nevi, and propensity to sunburn but not tan **(6)**. Inherited mutations in the *CDKN2A* and *CDK4* genes encoding the tumor-suppressor proteins p16 and p19, which have been documented in some families with hereditary melanoma, confer a 60 to 90 % lifetime risk of melanoma **(7, 8)**.

It is widely accepted that a person's total risk of melanoma is determined through the interplay between genetic factors and environmental factors, in particular exposure to sunlight **(3)**. The effects of solar radiation in melanoma development are nevertheless not clear. The existing evidence seems to implicate the activity of the mutagenic UV-B radiation (i.e. the one responsible for sunburn and tanning) as well as the proinflammatory, melanocyte activating effects of UV-A wavelengths (i.e. the one responsible for tanning). In addition, UV radiation has immuno-suppressive effects in the skin, thereby at least theoretically interfering with immunological mechanisms of cancer surveillance. Perhaps the clearest evidence for the tight relationship between UV exposure and the risk of melanoma development comes from a rare genetic disorder called xeroderma pigmentosum. Xeroderma pigmentosum is an autosomal recessive heritable condition characterized by molecular defects in the nucleotide excision repair of UV-B-induced DNA damage. Patients with xeroderma pigmentosum develop large numbers of non-melanoma skin cancers by early adulthood, and a subset of them are at high risk for melanoma development **(6)**.

4.1.3. Different subtypes of melanoma

There are four different subtypes of melanoma which are distinguished by clinical and histopathological features with distinct epidemiological parameters and particular patterns of mutation (**1**; Figure 3).

- *Superficial spreading melanoma (SSM)* - is the most common form of melanoma. It usually occurs in middle age but may appear in younger people too. In most cases it is flat with an intra-epidermal component and often with multiple colors and pale areas of regression.
- *Nodular melanoma (NM)* - most often occurs in middle age and is more frequent in males. It is an exophytic brown-black, often eroded or bleeding tumor, which consists of raised nodules. Nodular melanoma is characterized

by an aggressive vertical phase, with a short or absent horizontal growth phase. Due to this growth dynamics, its early identification in an intraepidermal stage is almost impossible.

- *Lentigo maligna melanoma (LM)* - usually occurs in older generation, most commonly on the face. It's usually flat in appearance, with dark brown or black color and is associated with lifetime chronic sun exposure.
- *Acral lentiginous melanoma (ALM)* - is most frequent type of this malignancy in non-Caucasian populations (e.g. Asians and Africans). It usually occurs on the palms of the hands, the soles of the feet and in the nail bed. The occurrence of this melanoma type is thus not associated with UV exposure **(1, 9, 10)**.

Figure 3 - Different subtypes of melanoma. 1 - Superficial spreading melanoma, 2 - Acral lentiginous melanoma, 3 - Lentigo maligna melanoma, 4 - Nodular melanoma. (http://courses.washington.edu/hubio567/melanoma/types.htm, adapted)

4.1.4. Diagnosis and staging

The large majority of persons diagnosed with melanoma are cured (> 85 %) due to the diagnosis at early stages of tumor development. On the other hand, melanoma can be highly malignant, because it is known to early metastasize to almost any organ in the body. Consequently, melanoma diagnosis at later stages of tumor progression is

associated with a poor prognosis. To assist physicians in early recognition of melanoma the ABCDE rule has been established:

- A = asymmetrical shape (melanoma lesions are often irregular or not symmetrical in shape)
- B = border irregularity
- C = color (the presence of more than one color can be a warning sign of melanoma)
- D = diameter (melanoma lesions are often greater than 6 millimetres in diameter)
- E = evolution **(6,11)**

Clinically, melanoma is classified into four stages referred to as TNM classification **(12)**. This classification describes the size and extent of the primary tumor - **T** (tumor), presence and extent of metastases in regional lymph nodes - **N** (nodule) and whether the melanoma has metastasized to distant organs- **M** (metastases) **(13)**.

According to histopathological stages, melanoma is also divided into 5 groups (0-IV). In situ melanomas (stage 0) are noninvasive without disturbed integrity of the epidermal basement membrane. Stage I and stage II melanomas are localized primary tumors without any regional or distant metastases. Stage III melanoma is characterized by regional spread through lymphatic vessels and in stage IV melanoma distant metastases are disseminated through hematogenous spread **(6)**.

In addition to the TNM classification, there is a Breslow histological evaluation where the depth of melanoma invasion into epidermis in millimetres is rated **(14)** or Clark's evaluation based on histological changes during the growth and progression of melanoma **(15)**. Together with presence of histologically recognized ulceration and mitotic rate, Breslow’s depth and Clark’s level belong to the most important histological prognosis factors for primary melanoma without metastases (**1**; Figure 4).

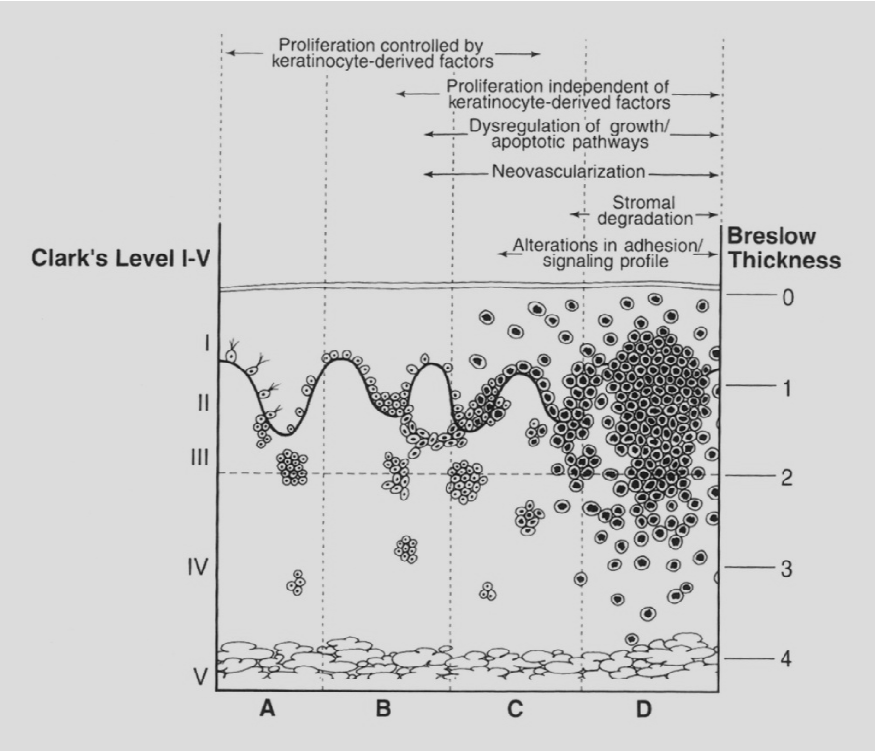

Figure 4 - Depth of invasion determined by Clark's level and Breslow thickness (Houghton, Alan N. and Polsky, David, 2002. Focus on melanoma. Cancer Cell. 2002. Vol. 2, no. 4, p. 277)

4.2. Melanocytes

Melanocytes are a heterogeneous group of pigmented cells occurring mostly but not only in the skin epidermis, hair and eyes. Their major function and characteristics is the production of the pigment melanin responsible for skin and hair colour **(9)**.

4.2.1. Evolution of melanocytes

Melanocytes differentiate from melanoblasts within the neural crest and then begin to migrate to stratum basale of the epidermis. Alternative pathways also lead them to hair follicles or to the uveal tract of the eye and the retina **(16)**. The homeostasis of melanocytes is regulated by epidermal keratinocytes **(17)**.

Melanocytes are oval, dendritic cells, smaller than keratinocytes. We can find them in the basal layer of epidermis where they, together with 30-40 associated keratinocytes, form the epidermal melanin units. In the epidermal basal layer the ratio of melanocytes to keratinocytes is about 1:10 and this ratio is maintained throughout the human life. In the epidermal melanin unit, the expression of the specialized adhesion molecules such

as E- and P-cadherins demonstrates the existence of close cell-to cell contacts. These contacts between the dendritic processes of differentiated melanocytes and keratinocytes are necessary for the melanin transfer into keratinocytes, which determines the skin color and confers photoprotection **(18)**.

4.2.2. Melanogenesis

Synthesis of melanin is a biochemical process called melanogenesis. It takes place in melanocytes, in separate cytoplasmatic organelles called melanosomes **(18)**. Melanosomes are large, lysosome-related organelles. They synthesize two kinds of melanin pigments: eumelanin and pheomelanin. Eumelanin is brown-black or dark insoluble polymer, which is found in dark skin and black hair, and pheomelanin is red-yellow soluble polymer connected to the red hair and freckled skin type. Both types of melanin show a different way of synthesis **(19, 20)**.

Melanogenesis is a complex process involving three enzymes: tyrosinase (TYR), tyrosinase-related protein-1 (TRP-1) and tyrosinase-related protein-2 (TRP-2 - otherwise known as dopachrome tautomerase, DCT), with TYR being absolutely necessary for melanogenesis**.**

The synthesis of melanin is initiated with hydroxylation of tyrosine to L-3,4-dihydroxyphenylalanine (DOPA) and catalyzed by the enzyme TYR (Figure 5). DOPA is then rapidly oxidized to DOPAquinone in the presence of TYR again. These two steps are common for both eu- and pheomelanogenesis pathways **(18, 19)**. Eumelanogenesis involves further transformation of DOPAquinone to DOPAchrome. The DOPAchrome spontaneously loses carboxylic acid with the production of the intermediates dihydroxyindole (DHI) and DHI-2-carboxylic acid (DHICA) in case the DCT enzyme is present. DHI and DHICA then undergo polymerization to form eumelanin. Pheomelanogenesis also starts with DOPAquinone, which reacts with cystein to yield cysteinylDOPA. CysteinylDOPA then oxidizes and polymerizes to be transformed into pheomelanin **(17, 18)**.

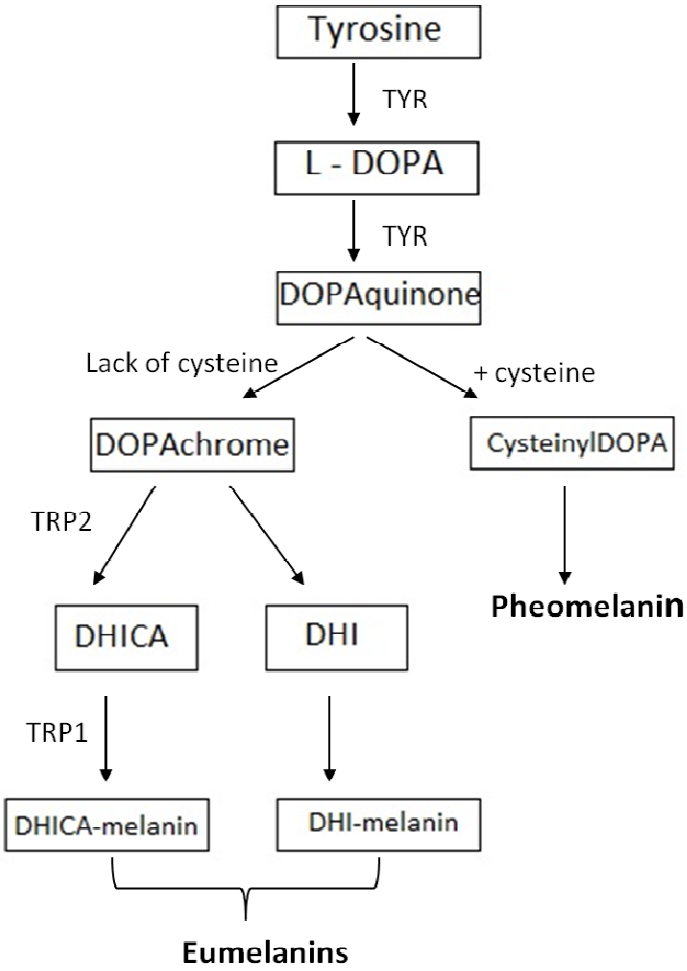

Figure 5 - Scheme of melanin synthesis during melanogenesis in melanocytes (Cichorek M. et al., 2013. Skin melanocytes: biology and development. *Advances in Dermatology and Allergology*. 2013. Vol. 30, no. 1, p. 34, adapted)

Human skin normally contains a mixture of all types of melanins and their ratio in part determines visible pigmentation **(21)**. The diversity of skin pigmentation among individuals from different ethnic groups is preserved in melanocytes cultured from individuals with different pigmentary phenotypes and depends on eumelanin content. In fact, it is the ratio of eumelanin to total melanin which decides about skin color whereas pheomelanin content does not appear to consistently correlate with skin pigmentation. Moreover, eumelanin is superior to pheomelanin in its photoprotective properties due to its higher resistance to degradation and its ability to reactive oxygen species neutralization **(22)**.

4.2.3. Regulation of melanogenesis

The synthesis of melanin is stimulated mainly by UV irradiation, which generates DNA photoproducts and leads to the release of various autocrine and paracrine factors. The most important factor secreted by keratinocytes is α-melanocyte-stimulating hormone (α-MSH). α-MSH is derived from its precursor proopiomelanocortin (POMC). The plasma membrane of skin melanocytes contains the melanocortin 1 receptor (MC1R) which is activated by α-MSH. This activation of MC1R receptor leads to stimulation of the expression of microphthalmia-associated transcription factor (MITF), which is essential for normal synthesis of melanin in melanocytes. The activity of MITF contributes to the expression of a host of genes that are involved in melanocyte survival, motility, differentiation, apoptosis and in melanosome production of tyrosinases **(20)**.

4.2.4. Melanocyte biology and transformation

The number, organization and biological activity of melanocytes in the epidermis are controlled and regulated by several genetic, epigenetic and environmental mechanisms whose interactions and full elucidation are still elusive. Melanocytes are highly differentiated cells characterized by a long life-span, increased resistance to environmental stresses and low proliferative activity. All aspects of this status are maintained via a complex interplay of diverse growth factors, paracrine factors and/or expression of cell surface molecules mediated by the interactions between melanocytes, keratinocytes, fibroblasts or other organs (e.g. pituitary gland) **(18)**. Furthermore, these "internal" players are under the influence of environmental factors, in particular UV radiation. UV radiation "activates" keratinocytes which secrete a series of factors to enhance melanocyte proliferation thought to be responsible for the formation of nevi. The melanocytes in a nevus do not significantly morphologically differ from normal melanocytes; however, they may start expressing growth factors and often harbor some genetic changes typical of fully developed melanoma **(23)**. Nevus cells stop proliferating at a certain stage to create a pigment cells population forming a mole **(24)**. This proliferation arrest is seemingly under the control of the cell cycle inhibitor $p16^{INK4A}$ as the defects in *CDNK2A* expression correlate with an increased number of moles and a higher risk of mole transformation **(25)**. Many moles/nevi never progress to further malignant stages to become melanoma and if so, this progress seems to be

highly individual with a gradual accumulation of genetic and epigenetic changes and a strong influence of microenvironment over linear or non-linear fashion **(23)**.

4.3. Genomic landscape of melanoma

According to The cancer genome atlas data, the mutation rate of melanoma is amongst the highest of all analysed malignancies **(26)**. The detailed enumeration of genetic and epigenetic changes detected in various forms of melanoma is beyond the scope of this introduction; however, some most commonly found genetic alterations are summarized in Figure 6.

Gene	Gene type	Alteration frequency/type(s) in melanoma
BRAF	Protooncogene	Mutation (50-70 %)
NRAS	Protooncogene	Mutation (10-30 %)
AKT3	Protooncogene	Overexpression
NF1	Tumor suppressor	Mutation (12-18 %)*
KIT	Protooncogene	Mutation (3 %), amplifications**
GNAQ	G protein	Mutation (1-2 %)**
GNA 11	G protein	Mutation (1-2 %)**
CDKNA2A	Tumor suppressor gene	Deletion, mutation or silencing (30-70 %)
PTEN	Tumor suppressor gene	Deletion or mutation (5-20 %)
APAF1	Tumor suppressor gene	Silencing (40 %)
Cyclin D1	Protooncogene (putative)	Amplification (6-44 %)
MITF	Transcription factor	Amplification (10-16 %)

Figure 6 - Selected genetic alterations in malignant melanoma (Gray-Schopfer et al., 2007. Melanoma biology and new targeted therapy. *Nature*. 22 2007. Vol. 445, no. 7130, p. 853. * Kiuru et al., 2017. The NF1 gene in tumor syndromes and melanoma. *Laboratory investigation; a journal of technical methods and pathology*. 2017. Vol. 97, no. 2, p. 146–157. ** Lyle et al., 2013. Diagnosis and treatment of KIT-mutant metastatic melanoma. *Journal of Clinical Oncology*. 2013. Vol. 31, no. 26, p. 3176–3181, adapted)

With increasing technical possibilities of genetic and epigenetic analysis (e.g. next generation sequencing), more detailed cataloguing of individual driver (signature) genetic changes is possible which has recently led to the proposed molecular classification of cutaneous melanoma into four genomic subtypes designated as *BRAF*, *RAS (N/H/K)*, *NF1*, and Triple-WT **(27)**. This proposed scheme endeavors to take into consideration not only general melanoma as such but also defined melanoma subtypes characterized by particular mutations: superficial spreading melanoma (SSM) and nodular melanoma (NM) which associate with *BRAF* or *NRAS* mutations; acral

lentiginous melanoma (ALM), lentigo maligna (LM), and mucosal melanoma that are more often positive for *KIT* mutations; and ocular melanomas often positive for *GNAQ* or *GNA11* alterations **(28)**. In addition, while individual genetic and epigenetic changes are extensively mapped and characterized, little is known about their succession and sequential order in melanoma evolution. To this end some recently published data formulate our first efforts to link melanomagenesis with the time frame of underlying molecular changes (**29, 30**; Figure 7).

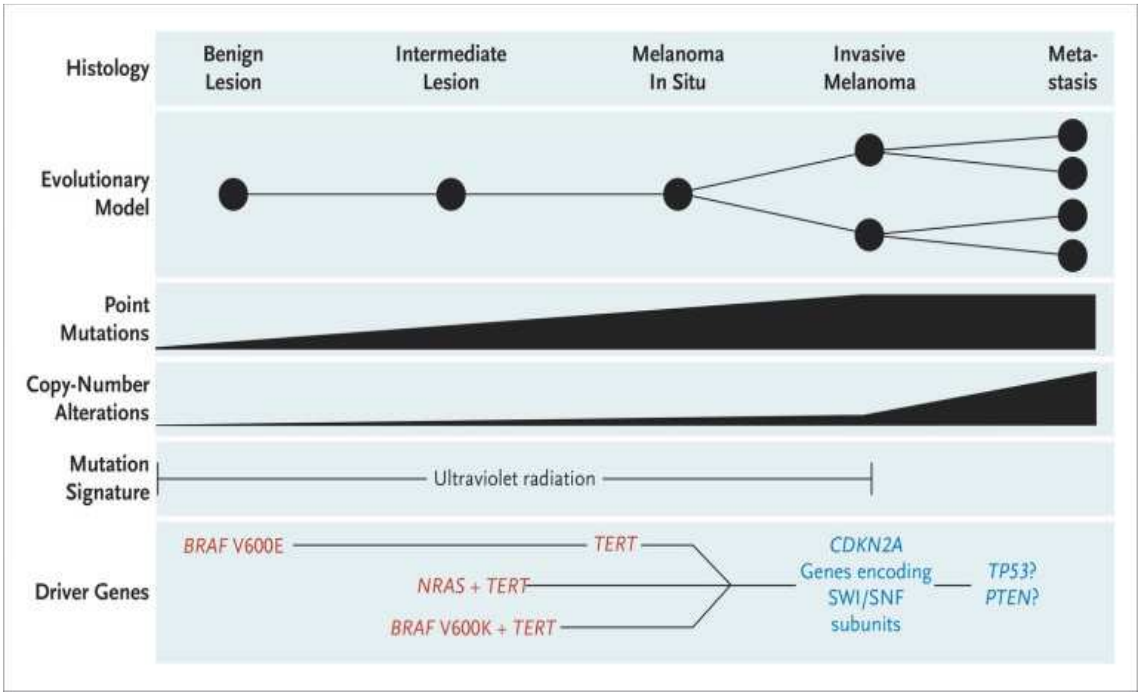

Figure 7 - Proposed models of sequential melanoma progression integrating molecular, evolutionary and histopathological data. (Shain, et al. 2015. The Genetic Evolution of Melanoma from Precursor Lesions. *New England Journal of Medicine*. 2015. Vol. 373, no. 20, p. 1934)

While some altered genes or genomic segments in concerned melanocytes often control generally known signaling pathways, others have a separate or unclear status and their involvement in particular signaling networks needs to be further specified. In the past, several key molecular pathways have been identified that are involved in melanoma onset, progression, and metastatic spread. Some crucial examples of these signaling pathways are stated below (Figure 8; for more comprehensive reviews see **(31, 32)**).

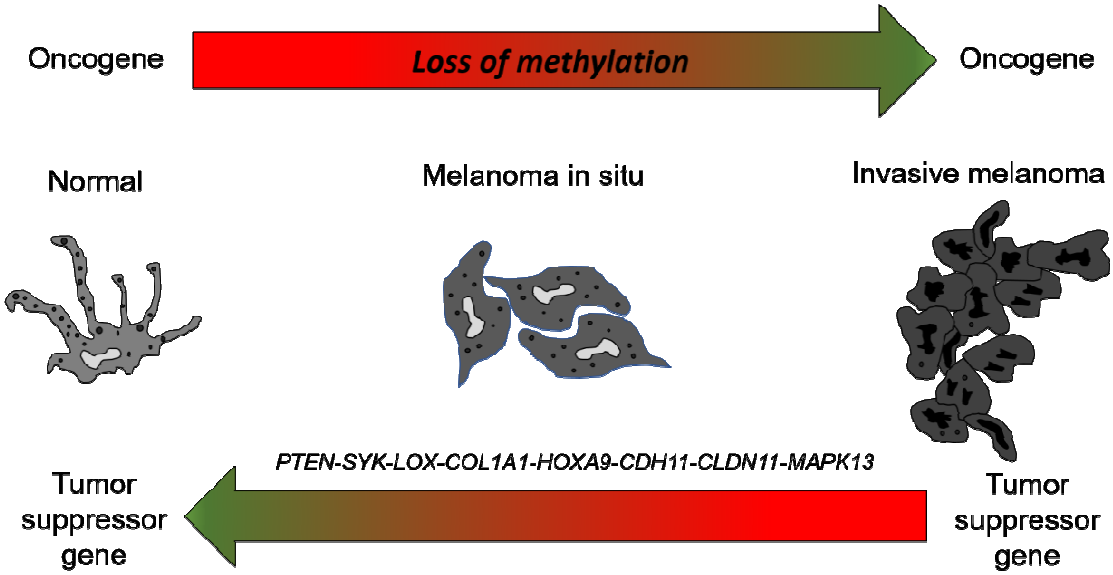

Figure 8 - Proposed sequential epigenetic changes in melanoma development. (Martinez-Cardus, et al.,2015. Epigenetic mechanisms involved in melanoma pathogenesis and chemoresistance. *Annals of Translational Medicine*. 2015. Vol. 3, no. 15, p. 209.)

4.3.1. RAS/RAF/MEK/ERK signalling

The RAS/RAF/MEK/ERK pathway is activated by growth factors in many cells including melanocytes and it is also a key regulator of melanoma cell proliferation. This mitogen activated protein kinase (MAPK) signaling pathway is regulated by receptor tyrosine kinases, cytokines and G-protein-coupled receptors. The transmission of signals is mediated via the membrane bound small G protein RAS GTPase which activates RAF (RAF-1, BRAF and ARAF) by complex events leading to MEK and ERK phosphorylation. The phosphorylated MEK and/or ERK translocate to the nucleus and regulate the expression of several transcription factors (*MITF*, *c-MYC*). Alternatively, MAPK signaling may increase the expression of cyclin D1 positively regulating cell cycle restriction checkpoint.

The RAS/RAF/MEK/ERK pathway is dysregulated in over 80 % of all cutaneous melanomas. It is due to activating mutations in several members of this pathway, most notably in *BRAF*, which is estimated to be mutated in 50-70 % of melanomas. More than 90 % of these mutations occur at codon 600, mostly as a single nucleotide mutation resulting in substitution of glutamic acid to valine (*BRAFV600E*). Other melanoma-linked mutations are found in the *NRAS* gene and occur in approximately 15-30 % of metastatic melanoma patients. *BRAF* and *NRAS* mutations stimulate constitutive

MEK-ERK signaling and lead to enhanced proliferation, survival, invasion and angiogenesis of melanoma **(9, 33)**.

4.3.2. PI3K/AKT pathway

The phosphatidylinositol-3-kinase (PI3K) pathway is involved in various physiological functions within the cell including cell growth, proliferation and metabolism. PI3K is known to occur in three classes, with the class 1 being the most characterized. Following its activation, this kinase catalyzes the production of a series of phospholipid derivatives functioning as second messengers to ultimately phosphorylate serine/threonine kinase AKT. AKT in turn is known to phosphorylate up to 100 target proteins and via various regulatory mechanisms elicits strong survival effects in the concerned cells. Upon physiological circumstances, this signalization is negatively regulated by PTEN (phosphatase and tensin homolog deleted on chromosome 10) induced dephosphorylation of second messengers resulting in reduced AKT levels and inhibition of P3IK signaling pathway.

Numerous studies have shown that PI3K/AKT pathway plays a rather important role in biology of melanoma and its therapeutic resistance. Uncontrolled activity of PI3K/AKT signaling is linked with *PTEN* loss/inactivation occurring in 10-30 % of melanoma and increased expression of AKT3 by gene amplification is found in about 60 % of sporadic melanomas **(23, 25, 26)**. *NRAS* and *PTEN* mutations were first reported to be mutually exclusive in melanoma, which is likely explained by their ability to share the same signaling pathway. However, recent data indicate that PI3K pathway mutations occur together with mutant *NRAS* in 9 % of tumors. Cooperation of *BRAF* and *PTEN* mutations was reported in 17 % of melanomas **(27)**.

4.3.3. WNT signalling

WNT (Wingless-related integration site) signaling controls several processes important in embryogenesis (cell fate, polarity) as well as in adulthood (proliferation, migration). WNT family glycoproteins bind to the extracellular receptor (seven transmembrane Frizzled – FZD) proteins to start three possible signaling pathways: a canonical β-catenin-dependent pathway, a non-canonical β-catenin-independent pathway and a WNT-dependent, protein kinase C (PKC)-dependent pathway. WNT signaling is crucial for the development of melanocytes from their neural crest

precursors and abnormal activation of the WNT pathway has been shown to play a key role in development of melanoma although details remain as yet unclear **(32)**. One known link might a gene Microphthalmia-associated transcription factor (*MITF*) encoding a transcription factor promoting survival in melanoblasts and driving melanocyte lineage commitment. *MITF* regulates the expression of melanogenic proteins such as tyrosinase, silver homologue (GP100) and melanoma-associated antigen recognized by T cells-1 (MART-1) and since it is expressed in most human melanomas its target genes are a diagnostic marker for this malignancy. Furthermore, stable, unrepressed *MITF* expression is essential for melanoma cell proliferation and survival **(9).**

Recent studies have shown that oncogenic BRAF may control intracellular levels of the MITF protein through a fine balance of two opposite mechanisms: a direct reduction of MITF levels, by inducing protein degradation, and an indirect increase of MITF levels, by stimulating transcription factors which increase protein expression levels. It has been shown that oncogenic *BRAF* mutations are associated with *MITF* amplification in a low fraction (10-15 %) of melanomas, suggesting that other mechanisms are likely to be involved in ERK-dependent degradation of *MITF* **(24).**

4.3.4. CDKN2/CDK4 tumor suppressive pathway

The *CDKN2A* is another major gene involved in melanoma pathogenesis and predisposition. It encodes two proteins, p16 and p14, both known as tumor suppressors. Proteins p16 and p14 are known as inhibitors of the cell cycle, which negatively interfere with the activity of the cyclin/CDK complexes and, in this way, ensure the control of the cell replication. The inactivation of *CDKN2A* is mostly due to point mutations (about 10 % of cases), genomic deletions (approximately 50 % of cases), or silencing. These mutations lead to the loss of the mechanisms controlling cell proliferation and / or survival **(33, 37)**.

4.3.5. p53 pathway

p53 regulates positively or negatively many genes involved in cell cycle regulation (*CDKN1A*), induction of autophagy, senescence, and apoptosis (*NOXA*, *PUMA*, and *BAX)*, as well as genes involved in the DNA repair or cellular metabolism. Mutations of *p53* are found in approximately 50 % of human cancers, but only sporadically and lately

in melanoma (about 10 % of cases). Why frequency of *p53* mutations is the lowest in melanomas compared to other malignancies remains to be solved **(33, 36)**. Although direct mutations in *p53* are infrequent in melanoma, inactivation of TP53 pathway occurs more via *CDKN2A* and loss-of-function of its product p14ARF **(33)**.

4.4. Chemoresistance

Chemoresistance or drug resistance of malignant cells is established as the primary cause of failure of chemotherapeutic treatment of most human tumors. Traditionally, chemoresistance is classified as intrinsic or acquired on the basis of the initial response to the first therapy with several pharmacological (e.g. tumor drug delivery, drug metabolism and selectivity etc.) as well as cellular (e.g. enhanced expression of drug efflux proteins, alterations in drug-targets, increased tolerance to stress conditions, and suppressed cell death signaling) mechanisms.

4.4.1. Chemoresistance in melanoma

Melanoma is an aggressive and multi chemoresistant type of malignancy with many of the above-mentioned drug-resistance mechanisms present inherently. Due to melanoma recognized intratumor heterogeneity, their presence is further linked with other transformation relevant features such as the epithelial-to-mesenchymal (EMT) transition and cancer cell stemness. Thus malignant melanocytes may develop a multi-drug resistance (MDR) phenotype related to overexpression of ATP-binding cassette (ABC) transporters, in particular ABCB5 **(29)** responsible for an efflux of a wide range of chemotherapeutics **(38)**. Conversely, the involvement of drug target alterations as well as the expression of detoxification enzymes in chemoresistance of melanoma continues to be controversial.

Given their natural role in superficial layers of our body, normal melanocytes are also endowed with enhanced survival mechanisms. These include for example increased expression of BCL-XL and MCL-1 antiapoptotic proteins which are also strongly expressed in all stages of melanomagenesis, thereby possibly contributing to melanoma resistance. In fact, based on the current evidence melanoma cells considerably rewire many sensors, regulators and effectors of apoptotic as well as nonapoptotic pathways **(38)**.

Other processes such as autophagy and its aberrant regulation play roles in melanoma survival too via so called autophagy paradox. This implies loss or deregulation of tumor suppressive autophagy in early stage malignancy and its upregulation in more advanced stages by helping melanoma cells escape drug-related toxicities **(39)**.

4.5. Treatment of malignant melanoma

4.5.1. Surgical therapy

The primary treatment of melanoma is surgical excision **(3)**, in particular wide excision, with either 1-2 cm margin of grossly normal tissue down to, but not including muscular fascia **(28)**. In patients with high-risk factors such as tumor thickness (depth greater than 4 mm), ulceration, high mitotic rate or regional node involvement, the risk of developing metastases can be very high (30-80 %) so systemic therapy is needed **(33)**.

4.5.2. Radiation therapy

Radiation therapy of the primary tumor is very rarely indicated; it is performed exclusively in patients in whom surgery is impossible or not reasonable **(3)**. This therapeutic approach is used for an uncommon type of melanoma known as desmoplastic melanoma or it can be used in combination with surgical therapy. Sometimes, radiation is given after surgery in the area where lymph nodes were removed or is used to relieve painful bone and brain metastasis. Treatment with the goal of relieving symptoms is called palliative therapy. Palliative radiation therapy is not expected to cure the cancer, but it might help shrink it or slow its growth for a time to help control some of the symptoms **(40)**.

4.5.3. Immunotherapy

It is mainly used as an adjuvant treatment for patients with primary melanoma stage II and III **(41)**. In immunotherapy two main molecules are used: interleukin-2 (IL-2) for advanced melanoma and the interferon alpha (IFNα) which is employed alone after surgery or in combination with other agents in advanced melanoma. However, treatment of melanoma patients with both immune system activating molecules failed to deliver

any clinically meaningful objective response rate and did not result in any improvement in overall survival as based on clinical trial evidence **(42)**.

4.5.4. Systemic therapy

The major indications for systemic therapy are inoperable regional and distant melanoma metastases (stage IV). Beside the standard cytostatic drugs, which were capable of inducing tumor responses but not of prolonging survival, new targeted compounds have been shown to prolong patient survival. The two main goals of systemic therapy are prolongation of survival and reduction of tumor size **(3)**.

4.5.4.1. Chemotherapy

Currently, no compound is known that would clearly improve patient prognosis. A number of agents with comparable effectiveness are available for systemic chemotherapy of advanced melanoma. The longest-established monotherapy is based on dacarbazine (DTIC) **(3)**. Treatment with DTIC alone or in combination has resulted in low response rates (about 10-20 %), rare durable responses with no impact on survival **(33)**. Temozolomide, an oral prodrug that yields the same active intermediate as dacarbazine, has been demonstrated to be as effective as DTIC, although more expensive. The antitumor activity of combinations of chemotherapeutic agents including cisplatin, vinblastine, dacarbazine and tamoxifen have failed to demonstrate a survival benefit compared with dacarbazine alone too **(41)**.

The combination of chemotherapy with immunotherapy resulted in increased response rates, however, survival benefit has not been demonstrated while toxicity was significantly increased **(33)**.

4.5.4.2. Targeted therapy

The increased knowledge about the molecular pathogenesis of melanoma has helped the research in the melanoma treatment. New agents used in melanoma treatment are the highly selective BRAF inhibitors (vemurafenib, dabrafenib), highly specific inhibitor of MEK (trametinib) or monoclonal antibody of anti-cytotoxic T-lymphocyte antigen 4, CTLA-4, (ipilimumab) **(33)**.

Furthermore, in 2015 talimogene laherparepvec (T-VEC, also known as OncoVEX^{GM-CSF}) became the first oncolytic virus approved for therapy in melanoma patients with injectable but non-resectable lesions in the skin and lymph nodes in the USA **(43)**.

Overall, targeted therapies have been clinically impactful for melanoma management, although they suffer from the drawback of resistance development after initial response or a lack of translation of target inhibition into disease control. The future of targeted therapies in melanoma management rests on successful translation of the understanding of the biological mechanisms of resistance into clinically significant therapeutic combinations **(44)**.

4.5.5. Novel approaches

Due to our constantly improving knowledge about molecular changes and corresponding biology of malignant tumors, novel pharmacological targets and approaches in oncological therapy are identified and tested. One such an approach is known as drug repurposing (repositioning); i.e. finding new indications of existing drugs **(45)**. This strategy holds a promising potential and to the date, in fact there are at least 46 approved drugs already repositioned for new therapeutic uses as indicated in literature **(46, 47)**. One example candidate chemical group for repurposing is benzimidazole derivatives.

4.6. Benzimidazole derivates

Benzimidazoles are the fused heterocyclic ring structures, which form an integral part of vitamin B_{12}. Substitution of benzimidazole nucleus has been shown to modify chemical and pharmacological properties of the structure and was a crucial step in the drug discovery process. The first benzimidazole to be developed and licensed for human use was thiabendazole in 1962 followed by a number of veterinary anthelminthics (parbendazole, fenbendazole, oxfendazole and cambendazole). The first benzimidazole carbamate used in humans was mebendazole, followed by flubendazole. Currently, some derivatives of benzimidazole are clinically approved including albendazole, mebendazole, thiabendazole as anthelmintics; omeprazole, lansoprazole, pantoprazole

as proton pump inhibitors; astemizole as antihistaminic; enviradine as antiviral; candesarten cilexitil and telmisartan as antihypertensives **(48)**.

4.6.1. Mechanism of action of benzimidazole carbamates

Benzimidazole carbamates specifically bind and interact with the β-tubulin subunit of microtubules **(49)**, despite the fact that their affinity for a mammalian tubulin is weaker than in helminths **(50)**. Since microtubule structures are very important for many vital functions of the parasite such as proliferation, mitosis, intracellular transport of organelles, maintenance of cell shape or cell locomotion, alteration of microtubular assembly and dynamics leads to the final destruction of the parasite **(49, 51, 52)**. In addition, benzimidazole carbamates may also inhibit energy metabolism of parasite cells. They cause disruption of transport and metabolism of glucose, resulting in energy and glycogen store depletion and loss of cellular motility. Even this process ultimately contributes to the death of the parasite **(53, 54)**.

4.6.2. Anticancer properties of benzimidazole carbamates

Benzimidazole carbamates interact with microtubules in helminths and were shown to bind with mammalian tubulin *in vitro*. This raised the question of whether this class of compounds could inhibit tubulin polymerization in human cells too and if so whether such a targeted effect could lead in a wider context to their antiproliferative and/ or antitumor effects in humans. First study to address this issue was published as early as in 1985. Still, more thorough inquiry into antiproliferative potential of benzimidazole carbamates was realized much more later. In a series of published studies, albendazole and mebendazole proved to be cytotoxic and cell death inducing compounds in a wide range of tumor cells as well as xenographt models **(46)**.

4.6.3. Flubendazole

Flubendazole (FLU) is a synthetic anthelmintic compound (Fig. 9), which was found by Janssen company in 1970s. In Europe, FLU is registered also for human use under the commercial name Fluvermal® for treatment of intestinal nematodes **(46)**.

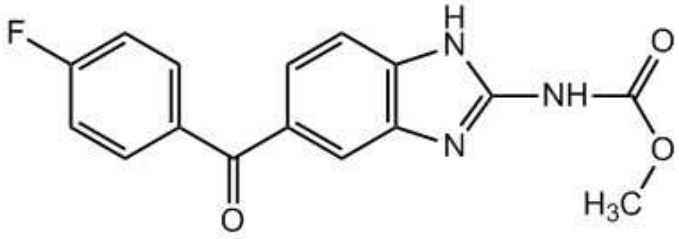

Figure 9 - Structure of flubendazole (FLU)

4.6.4. Anticancer effect of FLU

Anticancer activity of FLU was first reported in leukemia and myeloma cell lines where FLU inhibited cell growth and proliferation, arrested cell cycle and induced mitotic catastrophe. Similar effects were also observed in breast cancer cell lines MDA-MB-231, BT-549, MCF-7 and SK-BR-3 cells where in addition to classical inhibitory effects FLU induced cell differentiation and inhibited cell migration, which was accompanied by reduced expression of mesenchymal markers (β-catenin, N-cadherin and Vimentin) and induced expression of epithelial and differentiation marker (Keratin 18). In addition, FLU was described to be a potent inducer of reactive oxygen species (ROSs) capable of activating autophagy via targeting the autophagy-related protein 4B (ATG4B) **(46, 55)**.

In colorectal cancer cells SW480 and SW 620 FLU inhibited their growth, arrested them in G2/M phase and also potentiated the effect of paclitaxel **(56, 57)**.

Finally, in a screen of a panel of 321 cell lines including cell lines of various cancer types, neuroblastoma was identified as another highly FLU-sensitive malignancy type. The follow-up experiments proved that FLU displayed broad activity towards primary neuroblastoma cells obtained from five patients and a panel of 140 neuroblastoma cell lines with acquired drug resistance against major microtubule-binding compounds. The specific activity of FLU aimed p53-signalling and namely the protein PUMA which was demonstrated to be a key mediator of the induced effects **(46)**.

4.7. Mitotic catastrophe

In scientific literature, the term mitotic catastrophe is used to describe several related but not entirely identical phenomena. In particular, two opposing views are currently presented of whether mitotic catastrophe is a mode of cell death or whether it represents a series of steps leading to cell death (either apoptosis or necrosis) **(58)**. To this extent, mitotic catastrophe has been proposed to denote a form of cell death of mammalian cells resulting from abnormal mitotic process. In this concept, mitotic catastrophe is characterized by several distinct morphological features including the formation of large multinucleated cells with decondensed chromatin, overduplication of centrosomes and aberrant mitotic spindles. Moreover, some reports emphasize the presence of selected phenotypic features characteristic of apoptosis in cells undergoing mitotic catastrophe **(59)**.

An alternative view of mitotic catastrophe presents it as a sequential process culminating in cell death linked with mitosis. In this case, the process itself may be triggered by premature or aberrant entry of cells into mitosis due to the presence of inducing physical or chemical stressors. These stressors include DNA damaging agents such as doxorubicin or cisplatin, spindle poisons comprising both microtubule hyperpolymerizing (eg. taxanes, epothilones or eleutherobins) as well as depolymerizing agents (vinca alkaloids, cryptophicins or halichondrins) or inhibitors of mitotic proteins (monatrol or hesperidin). Their activities lead to defects in DNA (chromosomes) affecting their attachment to mitotic spindle, deranged spindle formation associated with defects in checkpoints or multipolar mitosis **(60)**. Based on the extent of damage, the length of spindle assembly checkpoint activation and the actual cell signaling context, final cell death phenotypes then might be reported autophagy, typical caspase-dependent apoptosis, or necrosis **(61, 62)**.

Despite the fact that cells undergoing mitotic catastrophe may potentially survive it and via so called mitotic slippage produce potentially dangerous progeny, in most cases mitotic catastrophe leads to cell death. Most malignant cells (including melanoma) show varying levels of genetic instability **(63, 64)**, and it was suggested that further stimulation of additional instability might represent a therapeutic strategy. Accordingly, malignant cells appear to be more susceptible to cell death following mitotic damage in comparison to nontransformed cells **(65)**, thereby making mitotic catastrophe a potentially important anticancer strategy which could achieved by a variety of mechanisms that target the cell cycle.

5. AIMS

In this work we set the following aims:

1. Determination of biological effects of FLU on normal human melanocytes

2. Investigation of cytotoxicity of FLU in the human malignant melanoma cell lines of differing molecular profile A-375, BOWES and RPMI-7951

3. Characterization of mechanisms whereby FLU induces its cytotoxic effects in the above mentioned cell lines, in particular with respect to mitotic catastrophe. Comparison of these effects with the ones known from other models

4. Obtaining and characterization of melanoma cells from patient samples and verification of FLU cytotoxicity

6. MATERIALS AND METHODS

6.1. Chemicals and reagents

Boehringer Mannheim-Roche:

WST-1 (4-[3-(4-iodophenyl)-2-(4-nitrophenyl)-2H-5-tetrazolio]-1,3-benzene disulphonate))

Cell Signaling Technology:

monoclonal rabbit anti-α-tubulin antibody, rabbit polyclonal anti-Bax antibody, polyclonal rabbit anti-p53, polyclonal rabbit anti-phospho-p53 (Ser15) antibody, Senescence β-Galactosidase Staining Kit #9860

DAKO:

Bcl-2 polyclonal antibody

Eli Lilly Czech Republic:

Humulin N 100 IU/ml

GIBCO:

penicillin, streptomycin, trypsin/EDTA, Medium 254CF, Human Melanocyte Growth Supplement (HMGS), Trypsin Neutralizer Solution

Invitrogen-Molecular Probes:

Click-iT® EdU Flow Cytometry Assay Kit, ProLong® Gold, MitoTracker, LysoTracker

LGC Standards:

Eagle's minimal essential medium (EMEM)

PAA Laboratories:

fetal bovine serum (FBS)

Promega:

Caspase-Glo® 2 assay, Caspase-Glo® 3/7 assay

RayBiotech:

Human/Mouse Phospho-p38 alpha (T180/Y182) ELISA

Santa Cruz Biotechnology:

rabbit polyclonal anti-p21 antibody

Sigma-Aldrich:

Dulbecco's Modified Eagle's Medium (DMEM), RPMI-1640 medium, dimethylsulfoxide (DMSO), 4-(2-hydroxyethyl)-1-piperazineethanesulfonic acid (HEPES) buffer, 4',6-diamidino-2-phenylindole (DAPI),

3[(3-cholamidopropyl)dimethylam-monio]-1-propanesulfonate hydrate (CHAPS), bicinchoninic acid (BCA) kit for protein determination, polyclonal mouse anti-β-actin antibody, Triton-X, flubendazole, bovine serum albumin (BSA), paraformaldehyde, transferrin 2mg/ml

Zentiva:

heparin 25,000 IU/ml

6.2. Cell lines

For our experiments we used normal human melanocytes, human malignant melanoma cell lines and melanoma cells derived from a patient´s sample obtained from Department of Plastic surgery, Faculty teaching hospital in Hradec Králové.

6.2.1. Normal human melanocytes

- **HEM-LP** (Fisher Scientific s.r.o. C0025C) human epidermal melanocytes are adherent cells isolated from neonatal foreskin from lightly pigmented tissue.

HEM-LP cell line was maintained in Medium 254CF, with added calcium chloride and Human Melanocyte Growth Supplement (HMGS), upon standard conditions (37 °C, 5% CO_2 in an incubator). The cells were passaged once a week using 0.05% EDTA/trypsin and the Trypsin neutralizer solution was added once the most of the cells were nearly completely round. The cells with Trypsin neutralizer solution were then transferred to a conical tube and centrifuged at 500 rpm for 5 minutes. The pellet was then resuspended with a fresh Medium 254 and 1/5 of suspension returned to the cultivation flask. The medium was changed every 2-3 days. Only mycoplasma-free cells were used for experiments.

6.2.2. Human malignant melanoma cell lines

We were using three different melanoma cell lines:

- **A-375** (ATCC® CRL1619™) are adherent, epithelial cells hypotriploid with a modal number of 62 chromosomes whose *BRAF* and *CDKN2A* genes are mutated.
- **BOWES** (ATCC® CRL9607™) are adherent, epithelial, heteroploid cells with wild-type *BRAF*.
- **RPMI-7951** (ATCC® HTB66™) are adherent, epithelial-like cells derived from metastasis to the lymph node, hyperdiploid (47-66 chromosomes) with mutant *BRAF*, *p53*, *CDKN2A* and *PTEN*.

A-375 and BOWES were maintained in DMEM medium supplemented with 10 % FBS and 1 % penicillin/streptomycin. RPMI-7951 was cultivated in EMEM medium with 10 % FBS and 1 % penicillin/streptomycin. Cells were maintained under standard laboratory conditions (37 °C, 5% CO_2) in an incubator and passaged twice a week upon reaching 90% confluence using 0.05 % EDTA/trypsin. Only mycoplasma-free cells were used for experiments.

6.2.3. Human explant melanoma cultures isolated from patients

Human dermal melanocytes were obtained from patients undergoing skin surgery at the Faculty teaching hospital in Hradec Králové. The study was approved by local ethics committee and in all cases tissues were obtained from subjects upon their informed consent.

Samples of a tumor tissue obtained by surgery were transported in a 50 ml tube with transport medium (RPMI-1640, 15 % foetal bovine serum, humulin N 100 IU/ml, transferrin, heparin) at room temperature to the Department of Medical biology and genetics where they were further processed. The tissue in the transport medium was placed on a Petri dish and cut into small pieces using scissors and a scalpel. Small pieces of the tissue were then collected with a Pasteur pipette and transported into cultivation flasks with cultivation medium (RPMI-1640, 1 % penicillin/streptomycin, 15 % FBS, humulin N 100 IU/ml, transferrin 2mg/ml). Samples were maintained upon standard conditions (37 °C, 5% CO_2) in an incubator and typically 48 hours post isolation individual cells appeared. The fresh medium was then added every 2-3 days

until most cells migrated from the tissue fragments and created monolayer on the bottom of the flask.

Cultures were subsequently passaged two times a week using 0.05 % trypsin/EDTA upon reaching 90 % confluence and cells were basically characterized.

During the entire study period, together 5 samples from 5 different patients were isolated and cultivated. In none of them detailed cell typing and sorting were carried out.

6.3. Stock solutions of FLU

Stock solutions of FLU were prepared in DMSO and stored in aliquots at 6 °C. Before experiments, FLU aliquots were diluted to the cultivation medium to achieve the following concentration range of FLU: 0.01 µM, 0.05 µM, 0.1 µM, 0.5 µM, 1 µM, 5 µM, 10 µM to which cell were subsequently exposed. The final concentration of DMSO in the medium was 0.1 %. Control samples were treated with a medium containing 0.1 % DMSO.

6.4. Determination of cell viability

Cell viability assays are based on the determined ratio of living and dead cells in the population. To measure cell viability, a number of methods may be used including direct microscopy observation and cell counting, determination of membrane integrity, measurement of metabolic activity or the rate of DNA synthesis.

6.4.1. The WST assay

This colorimetric assay is based on cleavage of WST-1 (4-[3-(4-iodophenyl)-2-(4-nitrophenyl)-2H-5-tetrazolio]-1,3-benzene disulphonate) by mitochondrial dehydrogenases to coloured and insoluble substance - formazan (Figure 10). Quantification of the formazan dye produced by metabolically active cells is measured with spectrophotometer and absorbance of the cleavage product correlates with the number of viable cells.

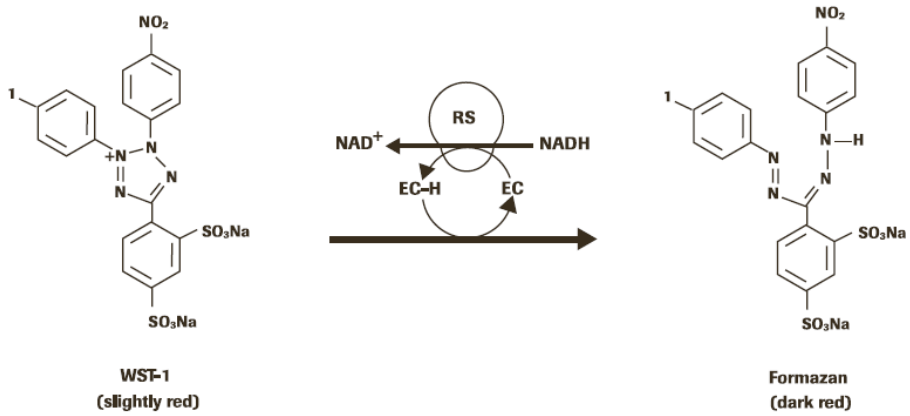

Figure 10 - Reduction of WST-1 to formazan (Roche diagnostic 2013, http://www.sigmaaldrich.com/content/dam/sigma-aldrich/docs/Roche/Bulletin/1/cellprorobul.pdf)

A-375, BOWES and RPMI-7951 melanoma cells were cultured in 96-well plates and treated with FLU at a concentration range of 0.01 µM – 10 µM. After 24-, 48- and 72-hours of exposure, the medium was removed and the cells were washed twice with 150 µl PBS. Then, 100 µl of culture medium containing WST-1 (0.3 mg/ml) was added to each well. Absorbance of the samples was measured immediately at 450nm / 650nm wavelength (Tecan Infinite M200; Tecan, Salzburg, Austria). The samples were then placed in the incubator and the absorbance was measured again after 2 hours of incubation. Each sample was assayed in 6 parallels and three independent experiments were performed. The viabilities of treated cells were expressed as a percentage of untreated controls (100 %).

Proliferation of HEM-LP cell line was examined at different cell seeding densities (100,000 cells/w, 50,000 cells/w, 20,000 cells/w) during different time intervals. WST-1 assay was performed as described above.

6.4.2. Test of proliferation using xCELLigence system

The system measures electrical impedance across interdigitated microelectrodes integrated at the bottom of tissue culture E-plates. The impedance measurement provides quantitative information about the biological status of the cells, including their number, viability and morphology.

At the beginning, 90 µl of culture medium were added into each well and plates were inserted in the device for background measurement. Then, 100 µl of cell suspension (containing 1,500 cells) were added in duplicate to the particular wells. The changes in impedance (corresponding to cell proliferation) were measured every 30 minutes for 24 hours. Next, 10 µl of treatment medium were added into each well, so that the final concentration of FLU corresponded to 1 µM. Plates were inserted back into the device and the impedance was measured every hour for total of 72 hours. Each sample was assayed in duplicate and three independent experiments were performed.

6.4.3. Microscopy-based cell counting

HEM-LP cells were cultured in small cultivation flasks and treated with 0.5 µM and 1 µM FLU. Numbers of living cells were counted with a phase-contrast microscope Nikon Eclipse E 400 (Nikon, Prague, Czech Republic) during a 24-96 hours interval. Photographs of cultures melanocytes were acquired using software LUCIA DI Image Analysis System LIM (Laboratory Imaging Ltd., Prague, Czech Republic), software processed and analysed. For the purpose of analysis, the minimum 2,000 cells were evaluated at 100x and 400x magnification. A total of six independent experiments were performed.

6.5. Time-lapse videomicroscopy

A-375, BOWES and RPMI-7951 melanoma cell lines as well as HEM-LP cells and patient´s melanoma cultivations were individually seeded into plastic tissue-culture dishes with glass bottom and left for 24 hours in an incubator with 5% CO_2 at 37 °C. Next, the growth medium was replaced with a medium containing FLU at a concentration of 1 µM. The tissue-culture dishes were transferred into a time-lapse imaging system BioStation IM (Nikon, Prague, Czech Republic) combining an incubator, a motorized microscope and a cooled CCD camera. Recording was carried out in a multipoint and multichannel manner employing various time-lapse modes and upon small as well as high magnifications to allow global as well as detailed view of changes in behaviour of treated cell populations. Recorded sequences were subsequently semi automatically analysed with the software NIS Elements AR 3.20 (Nikon, Prague, Czech Republic).

6.6. Cell cycle distribution analysis

6.6.1. Flow cytometry

A-375, BOWES and RPMI-7951 melanoma cells were cultured in 75 cm^2 culture flasks in 20 ml of culture medium for 12 and 24 hours. Then the culture medium was replaced by a fresh medium containing 1 µM of FLU or 0.1 % DMSO as a control. After 12 or 24 hours of treatment, the cells were trypsinized, collected by centrifugation, washed with PBS and fixed with ice-cold 70% ethanol while gently vortexing. Fixed samples were stored overnight at 4 °C. Next, they were washed with PBS and incubated with 0.5 ml of the Vindelov solution (1.2 g/l TRIS, 0.6 g/l NyCl, 0.01 g/l RNase and 0.05 g/l propidium iodide) for 50 minutes at 37 °C. Thus processed samples were analysed with the FC500 Cytomics Flow cytometer (Beckman Coulter, Hialeah, FL, USA) with PI fluorescence detected in FL3 channel. Cell cycle distributions in control and treated samples were analysed with MultiCycle AV for Windows (Phoenix Flow Systems, San Diego, USA). Three independent experiments were performed.

6.6.2. Percentage of cells in S-phase by EdU labelling

EdU (5-ethynyl-2´-deoxyuridine) is incorporated into DNA during active DNA synthesis. A-375, BOWES and RPMI-7951 melanoma cells were cultured in 96-well plates and treated with FLU at a concentration of 1 µM. After 24 hours exposure, the cells were labelled with EdU (Click-iT® EdU Flow Cytometry Assay Kit) at a concentration of 10 µM and incubated for 2 hours. After EdU labelling the medium was removed and the cells were washed in PBS and fixed with freshly prepared paraformaldehyde (4%) and incubated for 15 minutes. After incubation, there were washed again with PBS + 3% BSA and permeabilized with 0.5% Triton-X for 20 minutes at room temperature. After detachment of permeabilization solution, cells were washed twice in PBS + 3% BSA and EdU buffer additive was added to the plates followed by further incubation (30 minutes in the dark). About 5 minutes before the end of incubation DNA-specific solution DAPI (1 µg/ml) was added to the cells. Cells were washed again and finally scored using Image Xpress Micro XLS Widefield High-Content Analysis System. Specific fluorescence was visualized, recorded and analysed by Cell scoring module of MetaXpress® Image Acquisition and Analysis Software

(Molecular Devices, Sunnyvale, CA, USA). Three independent experiments were performed.

6.7. Fluorescent visualisation of mitochondria and lysosomes

A-375, BOWES and RPMI-7951 melanoma cells were seeded in cytospin chambers and allowed to grow overnight at 37 °C. In control cells or in cells treated with 1 μM FLU, slides with grown cells were rinsed in a warm medium and stained with MitoTracker Green FM (100 nM, 30 minutes, 37 °C), LysoTracker Red (30 nM, 30 minutes, 37 °C) and Hoechst 33528 (10 nM, 30 minutes, 37 °C). Following another rinsing with warm cultivation medium, specimens were mounted and mitochondria and lysosomes in individual cells were assessed by an epifluorescence motorized microscope Nikon Eclipse E 400 (Nikon Corporation, Japan) equipped with a digital color matrix camera COOL 1300 (VDS, Vosskűhler, Germany), using a FITC, TRITC and DAPI specific filters**.** Resulting images were analysed by the software LUCIA DI Image Analysis System LIM (Laboratory Imaging Ltd., Prague, Czech Republic). All experiments were repeated at least three times.

6.8. Caspase assay

The activities of caspases 2 and 3/7 were assayed using Promega Caspase-Glo Assay. A-375, BOWES and RPMI-7951 melanoma cells were cultivated in 96-well plates. After 12, 24 and 48 hours incubation of cells in the medium containing 1 μM FLU, cells were lysed using buffer containing 50 mM HEPES, 5 mM CHAPS, 5 mM DTT. Then the lysates were collected into microtubes. Caspases 2 and 3/7 reagents were prepared as described in manufacturer's instruction. The lysates (25 μl in each well) were transferred into white-walled 384-well-plates for luminometer. Then, 25 μl of Caspase 2 or Caspase 3/7 reagents were added to each well. The plate was gently mixed for 30 seconds and then incubated for 30 minutes at room temperature. The luminescence was measured in three independent experiments using luminometer (Tecan Infinite M200; Tecan, Salzburg, Austria).

6.9. Immunofluorescence and image analysis

A-375, BOWES and RPMI-7951 melanoma cells in cytospine chambers were exposed to 1 µM FLU for 12 and 24 hours, then were washed by 1 ml pre-warm PBS and fixed with 4% paraformaldehyde (10 minutes, 25 °C), rinsed with phosphate saline buffer with 1% Triton X (PBS-T) and blocked in 5% BSA for 1 hour at 25 °C. Incubation was performed at 4 °C for 1 hour using α-tubulin (1: 100), ß-actin (1:1,000) and p21 (1:100) primary antibodies. After washing with cold PBS (5 minutes, 25 °C), secondary antibody (anti-rabbit/anti-mouse, 1:250) was added for additional 1 hour (25 °C). The specimens were then rinsed three times in PBS, post-labelled with DAPI (10 µg/ml, 15 minutes, 25 °C), mounted into ProLong® Gold medium and examined under fluorescence microscope Nikon Eclipse E 400 (Nikon, Prague, Czech Republic) (excitation filter 330-380 nm and emission filter 420 nm) equipped with a digital color matrix camera COOL 1300 (VDS, Vosskűhler, Germany). Photographs were taken using the software NIS Elements AR 3.20. Samples were prepared in duplicates, three independent experiments were performed.

6.10. Western blot analysis

Treated and control cells were washed with PBS and harvested in ice-cold lysis buffer (50 mM Tris/HCl, 150 mM NaCl, 10% glycerol, 1% Triton X-100, 2 mM EDTA, 2 mM EGTA, b-glycerolphosphate, 50 mM NaF, 10 mM sodium pyrophosphate, 200 lM sodium orthovanadate, 2 mM DTT). The lysates were resuspended and supernatants were obtained after a 13,000 rpm centrifugation at 4 °C for 10 minutes. Amount of protein in supernatant was determined by BCA assay. The SDS sample buffer (Tris–HCl pH 6.8, 40% glycerol, 6% SDS, 0.2 M DTT, 0.1 g bromphenol blue) and lysis buffer were added according to BCA assay results to obtain the same protein concentration of all the samples. Fifteen micrograms of protein were separated on 10 % or 15 % (based on protein size) polyacrylamide gels. After electrophoresis (15mA per gel, 200V, 75 minutes), proteins were transferred to a PVDF membrane (170 mA, 25V, 20 minutes for 1 gel) and blocked for 1 hour with 5% nonfat dry milk in TBST (Tris-buffered saline containing 0.05% Tween 20). Then, the membranes were incubated with primary antibody overnight at 4 °C with gentle shaking. These conditions were applied for detection of BAX (polyclonal rabbit antibody, 1:1,000), TP53 (polyclonal rabbit antibody, 1:1,000) and phospho-TP53 (ser15) (polyclonal rabbit antibody, 1:1,000).

In case of β-actin (polyclonal mouse antibody, 1:8,000) and BCL2 (polyclonal mouse antibody, 1:400), the incubation with the primary antibody lasted for 1 hour at room temperature. Subsequently, the membranes were washed six times in TBST for 9 minutes, followed by 1 hour incubation with a secondary antibody at room temperature (anti-rabbit secondary antibody, 1:2,000 for BAX, TP53 and phospho-TP53 (ser15), and anti-mouse secondary antibody 1:800 for BCL2 and 1:10,000 for β-actin). After washing the membrane six times (9 minutes) with TBST, the chemiluminescence process and quantification of immunoreactive bands on the exposed films were carried out using the QuantityOne imaging software (Bio-Rad Laboratories, Hercules, CA). For each antibody used, three independent experiments were performed.

6.11. Statistics

Statistical analysis was carried out with a statistical program GraphPad Prism (GraphPad Software version 6.0, Inc. San Diego, U.S.A.). We used one-way Anova test and two-way Anova with Bonferroni's test for multiple comparisons.

7. RESULTS

7.1. Antiproliferative effects of FLU in different melanoma cell lines

The effect of FLU at a concentration range of 0.01 – 10 µM on viability and proliferation of three human melanoma cell lines A-375, BOWES and RPMI-7951 during up to 72 hours of exposure was evaluated with formazan assay WST-1. In all three cell lines FLU showed a concentration and time-dependent cytotoxicity.

In A-375 cells, the earliest statistically significant observable inhibition of viability and proliferation was seen after treatment with 5 µM FLU (24 hours of exposure). After 48 hours treatment interval, the inhibitory FLU concentration was 1 µM and at 72 hours of exposure the same antiproliferative effects were achieved with 0.1 µM FLU (Fig. 11).

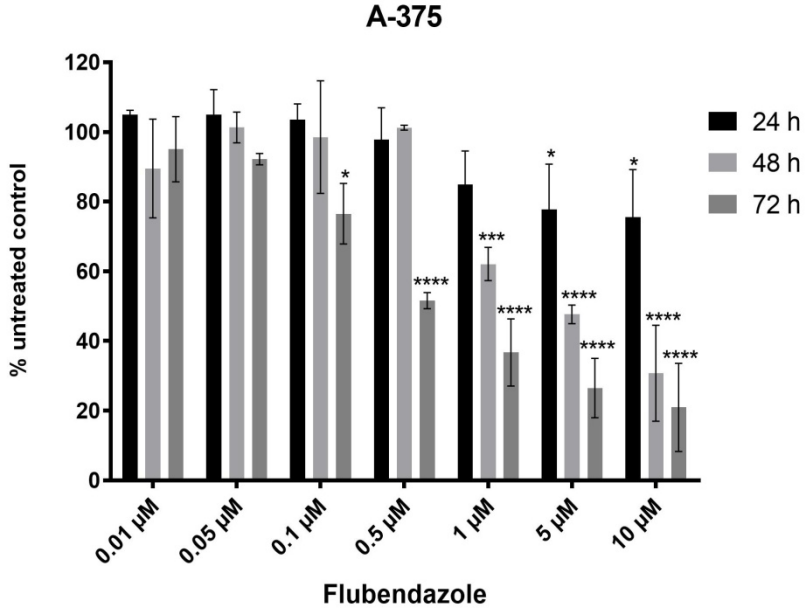

Figure 11 - Proliferation of A-375 cells treated with flubendazole (FLU) at concentration range 0.01 - 10 µM as measured by WST-1 assay. The data represent mean ± SD from three independent experiments. * P < 0.05, *** P < 0.001, **** P < 0.0001

In the employed experimental conditions, BOWES cell line proved to be of different sensitivity. After 24 hours of exposure, the first statistically significant inhibition occurred with 1 µM FLU. On the other hand, during longer treatment intervals of 48 hours and 72 hours, the inhibitory FLU concentration was lower and corresponded to 0.5 µM (Fig. 12).

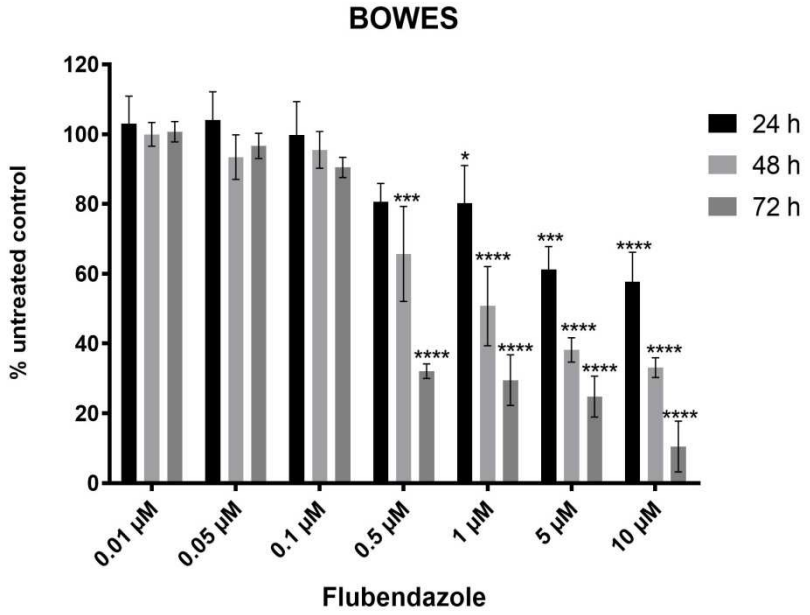

Figure 12 - Proliferation of BOWES cells treated with flubendazole (FLU) at concentration range 0.01 - 10 µM as measured by WST-1 assay. The data represent mean ± SD from three independent experiments. * P < 0.05, *** P < 0.001, **** P < 0.0001

The sensitivity of RPMI-7951 cells to FLU treatment did not significantly differ from the one verified with other two tested cell lines (A-375 and BOWES). Still, while FLU at the concentration of 0.5 µM markedly suppressed viability and proliferation of these melanoma cells at 72 hours of treatment only, the concentration of 1 µM proved to be cytotoxic at both earlier time intervals (i.e. 24 hours and 48 hours) (Fig. 13).

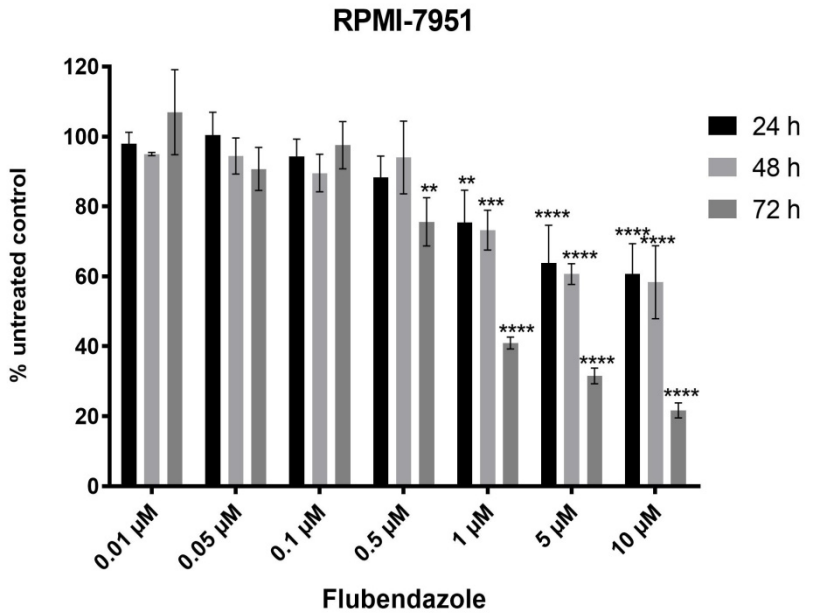

Figure 13 - Proliferation of RPMI-7951 cells treated with flubendazole (FLU) at concentration range 0.01 - 10 µM as measured by WST-1 assay. The data represent mean ± SD from three independent experiments. ** P < 0.01, *** P < 0.001, **** P < 0.0001

Subsequent experiments using xCELLigence system confirmed these observations and helped to determine FLU IC_{50} values for each model cell line: A375 - IC_{50} = 0.96 µM (Fig. 14A), BOWES - IC_{50} = 0.90 µM (Fig. 14B) and RPMI-7951 - IC_{50} = 0.25 µM (Fig. 14C). In view of these results, the FLU concentration of 1 µM was used for subsequent experiments.

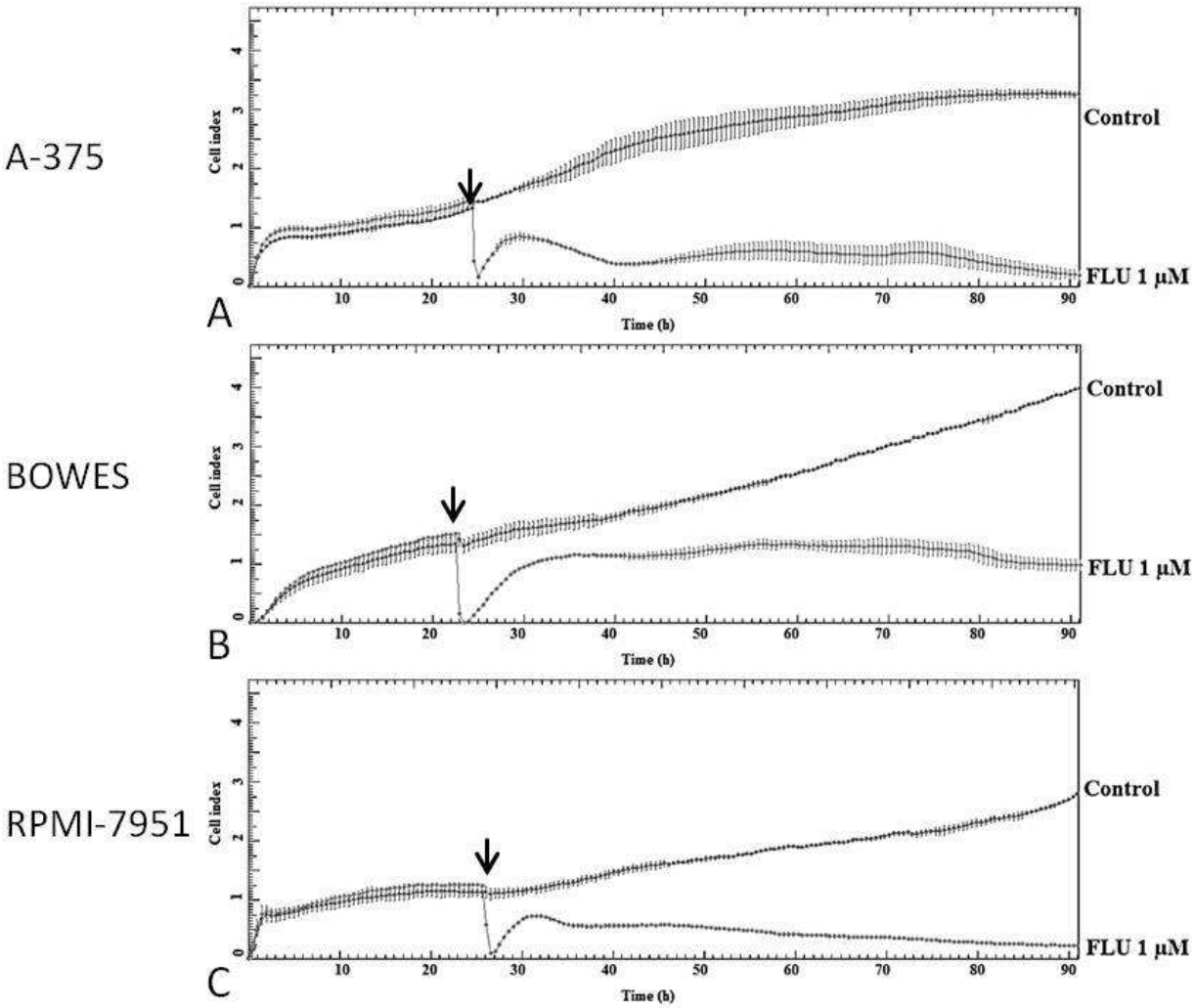

Figure 14 - Proliferation of A-375, BOWES and RPMI-7951 cells exposed to flubendazole (FLU) as measured by real-time xCELLigence system. The arrow represents the treatment after 24 hours of proliferation.

7.2. Antiproliferative effects of FLU in normal human melanocytes

Prior to further studies into the mechanisms of cytotoxicity of FLU in the employed melanoma cell lines, the potential cytotoxic effects of the chosen 1 µM FLU concentration were assessed in normal human melanocytes HEM-LP.

7.2.1. Basic growth characteristics of HEM-LP

Human epidermal melanocytes HEM-LP have typical melanocyte morphology, i.e. a multipolar shape with numerous spike-like extensions, larger nuclei and less conspicuous lysosomes and melanosomes. They grow as adherent cells in

a multi-layered fashion and show motile activity. Their proliferation and cycling are slow (population doubling occurs in the range of 4 and more days) and clearly depend on several factors such as seeding density as confirmed by our initial observations using WST-1 assay and time-lapse studies (Fig. 15).

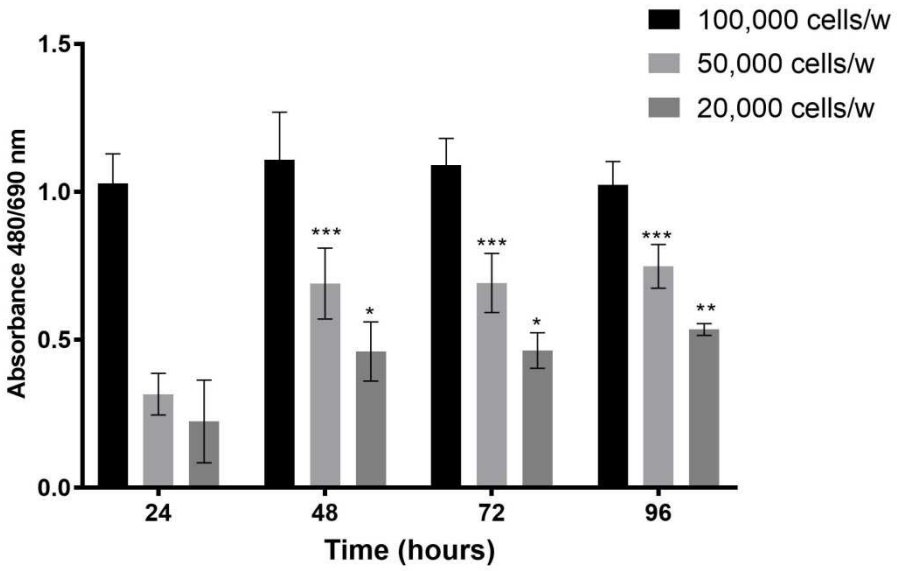

Figure 15 - Proliferation of HEM-LP cells as measured by WST-1 assay. The data represent mean ± SD from three independent experiments. * P < 0.05, ** P < 0.01, *** P < 0.001

7.2.2. Cytotoxicity of FLU on HEM-LP

Due to the slow growth and proliferation of HEM-LP cells with further dependence on cell seeding density, which could produce potentially inconsistent data from WST-1 assay, we chose to evaluate FLU effects on these cells using a direct microscopy-based software aided cell counting. In control cultures, the entire population doubling did not occur during the followed 96 hour interval; however, a steady increase in the number of cells was noted which was most dramatic during 24-48 hours interval. The addition of 1 µM FLU resulted in a decreased rate of cell proliferation observable throughout the entire treatment period. Similar trend albeit with a lesser proliferation suppression in HEM-LP cells was also recorded in case of lower FLU concentration of 0.5 µM (Fig. 16).

On a qualitative level, the addition of 1 µM FLU produced an immediate change in HEM-LP morphology and behaviour. Cells rapidly retracted their extensions, became more flattened and filled up with numerous small vesicles resembling vacuoles. Some of them underwent rapid shrinkage and degradation, in particular during first 12-24

hours of exposure. The rate of cell demise was not; however, too high and most exposed cells survived and continued in their existence. During later treatment periods (72–96 hours), exposed cells started to gradually change again back to their original morphological appearance and behaviour. This transition was accompanied by partial disappearance of cytoplasmic vesicles, resumed motile activity and overall patterning of cell population (Fig. 17). These data collectively demonstrate that FLU at the concentration of 1 μM has some cytotoxic and cytostatic effects in normal human dermal melanocytes HEM-LP but these effects seems to lessen during the time and most exposed cells may tolerate them.

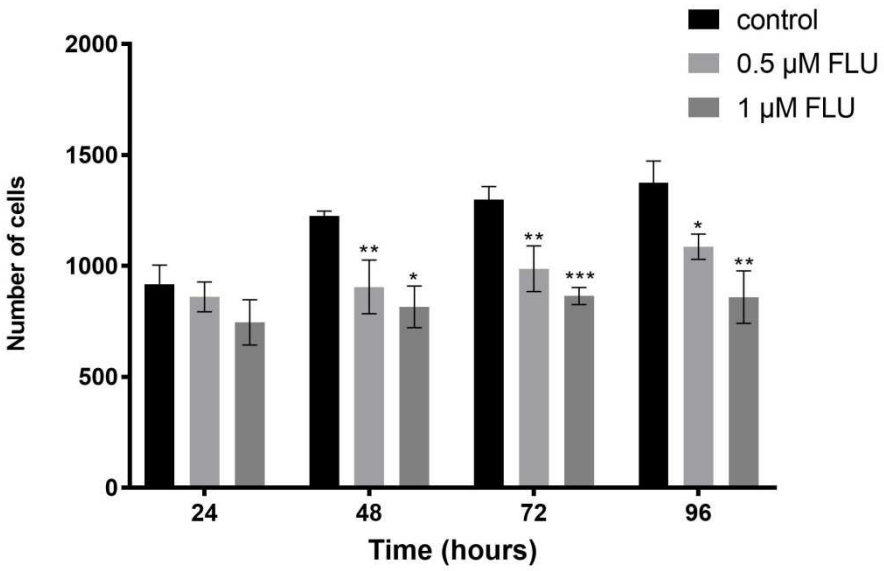

Figure 16 - Proliferation of HEM-LP cells exposed to differing concentrations of flubendazole (FLU) during 96 hours as determined by cell counting. The data represent mean ± SD from three independent experiments. * $P < 0.05$, ** $P < 0.01$, *** $P < 0.001$

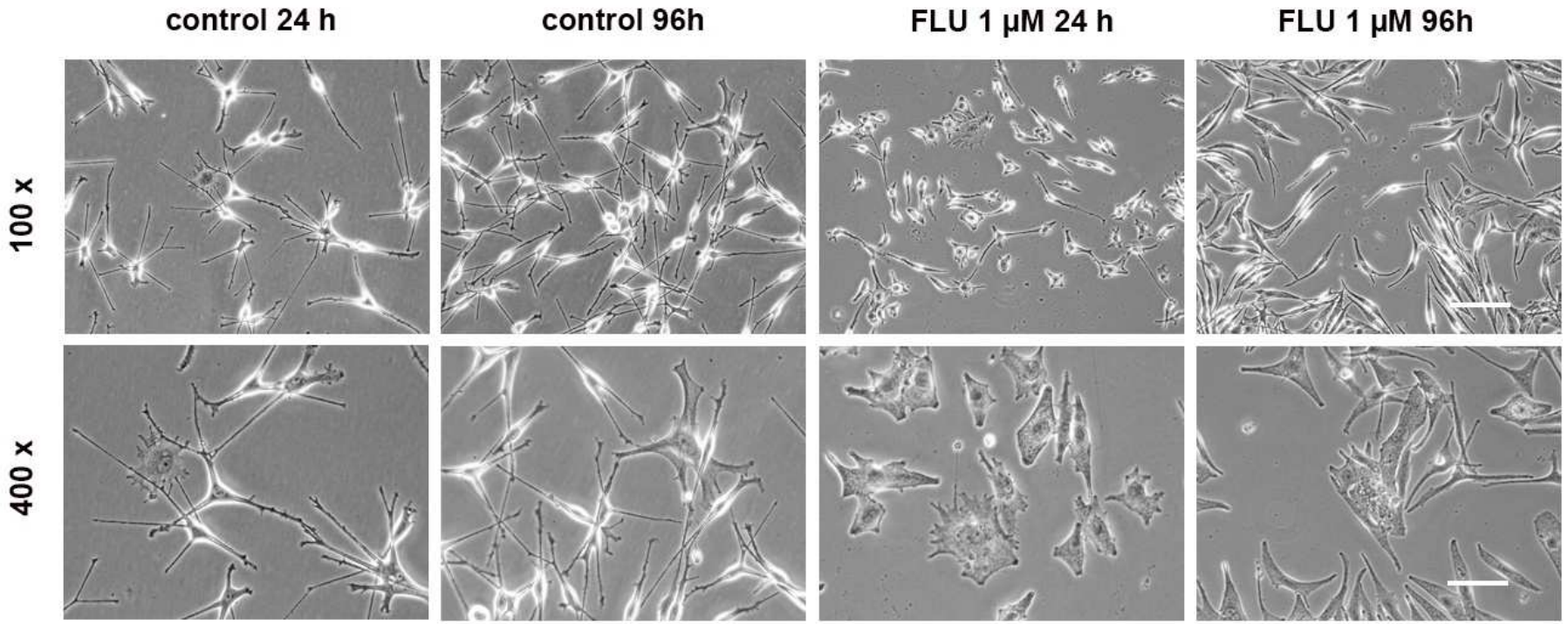

Figure 17 - Morphology of human normal melanocytes HEM-LP during 96 hours of exposure to1 µM flubendazole (FLU). Phase contrast 100 x and 400 x. Scale 30 µm.

7.3. Effects of FLU treatment on cell cycle distribution

Flubendazole at the concentration of 1 µM showed antiproliferative effects in the employed melanoma cell lines while its cytotoxicity was much better tolerated in normal melanocytes. Thus to gain further insight into mechanisms underlying FLU-dependent cytotoxicity in melanoma cells, cell cycle analysis with help of flow cytometry was next carried out. In FLU-exposed cell populations, as early as at 12 hours after the beginning of treatment, significant changes in particular cell cycle phases were recorded when compared to controls. While individually varying, these changes were still present in all three tested cell lines. Universally, both G1 and S phase cells declined in their numbers, with a marked increase in G2/M fraction cells (Fig. 18B). This trend continued into 24 hours treatment interval and resulted in the majority of cells accumulated in G2/M phase. In A-375 cell line 79 % of cells were accumulated in G2/M phase, while only 2 % in G1. In BOWES cell line 75 % cells were in G2/M and only 9 % in G1 and in RPMI-7951 cell line 71 % of cells were in G2/M phase and 15 % in G1 phase (Fig. 18A). Furthermore, another independent analysis using EdU labelling assay demonstrated that FLU treatment had a similarly severe effect on S phase cells too. In A-375 cell line S phase cells dropped to 8 % compared to approximately 50 % in controls, in BOWES cell line S phase cells dropped to 11 % compared to approximately 40 % in controls. In RPMI-7951 only S phase cells numbers were reduced to just 25 % compared to approximately 45 % in controls; however, even this difference was statistically significant (Fig. 19).

7.4. Effects of FLU treatment on cell cycle inhibition

In order to verify the molecular nature of our observed G2/M phase block in melanoma cells induced by 1 µM FLU, an analysis of cell-cycle inhibitors expression was carried out. Out of all potential cell cycle inhibitors belonging to INK4 and CIP/KIP protein families, the expression of p21 inhibitor protein was selected due to its role in both G1 and G2/M induced cell cycle blocks. Immunofluorescent detection of p21 protein in control cells revealed its weak presence and expression namely in the nuclei of melanoma cells. Treatment with 1 µM FLU induced increased expression of p21 as evident from its positive staining in the treated cell nuclei as well as cytoplasms at both time intervals of 12 hours and 24 hours. This effect was universal and no

quantitative as well as qualitative changes in the p21 protein presence were noted in all the employed cell lines (Fig. 20).

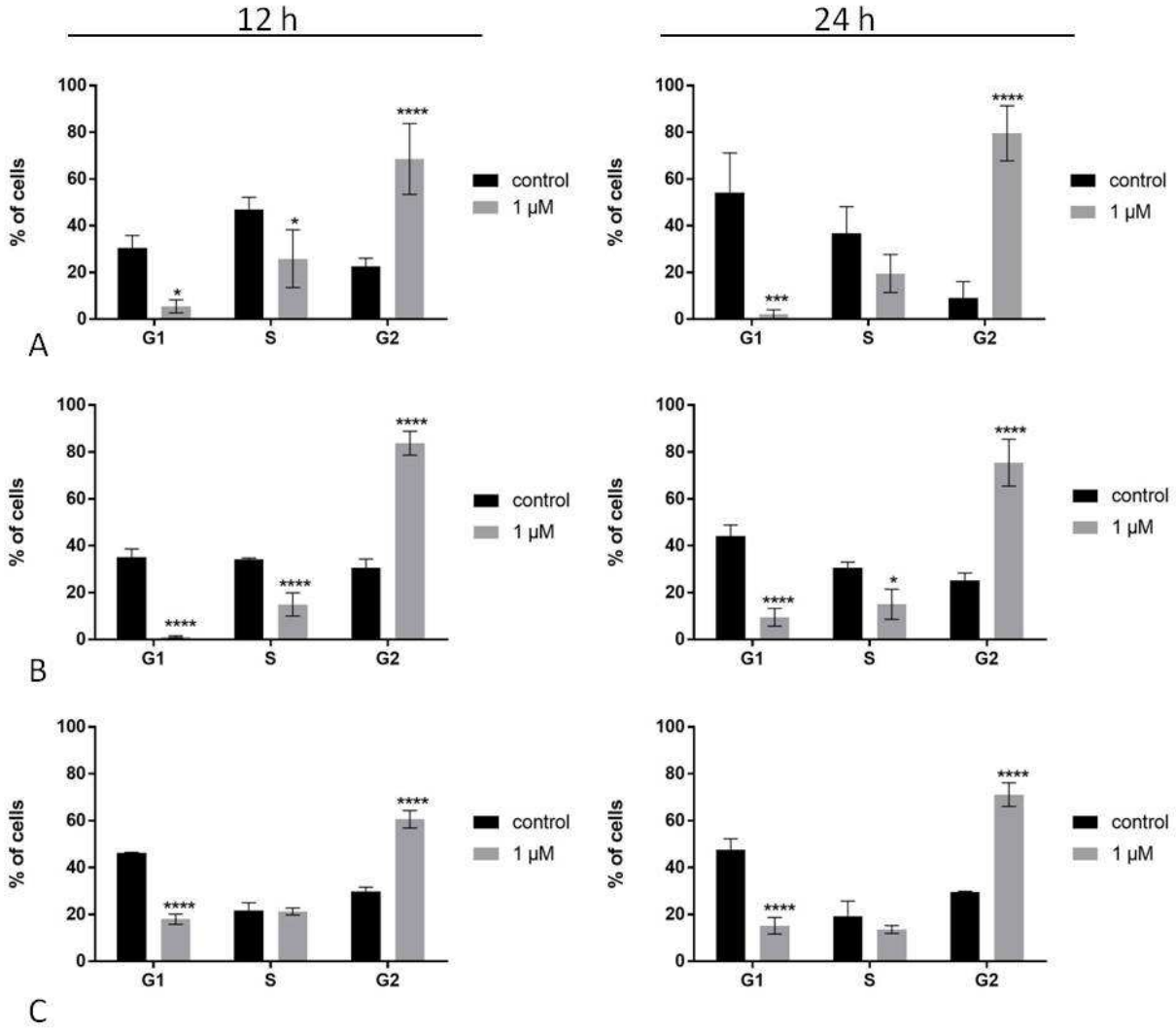

Figure 18A - Cell cycle changes in melanoma cells A-375, BOWES and RPMI-7951 exposed to 1 μM flubendazole (FLU) during 24 hours as measured by flow cytometry. A. A-375 at 12 hours and 24 hours treatment with FLU. B. BOWES at 12 hours and 24 hours treatment with FLU. C. RPMI-7951 at 12 hours and 24 hours treatment with FLU. The data represent mean ± SD from three independent experiments. * $P < 0.05$, *** $P < 0.001$, **** $P < 0.0001$

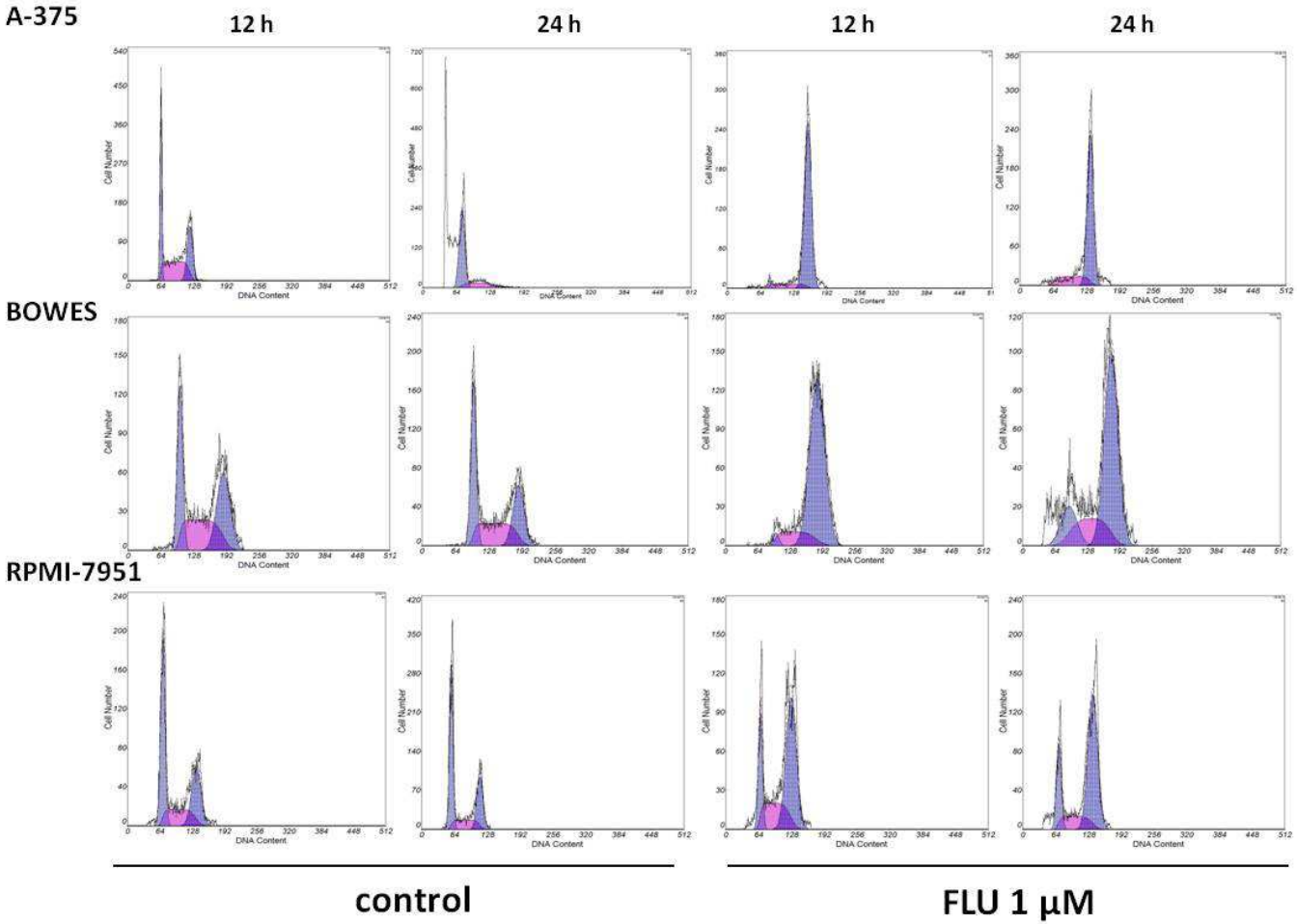

Figure 18B - Cell cycle changes in melanoma cells A-375, BOWES and RPMI-7951 exposed to 1 µM flubendazole (FLU) during 24 hours as measured by flow cytometry.

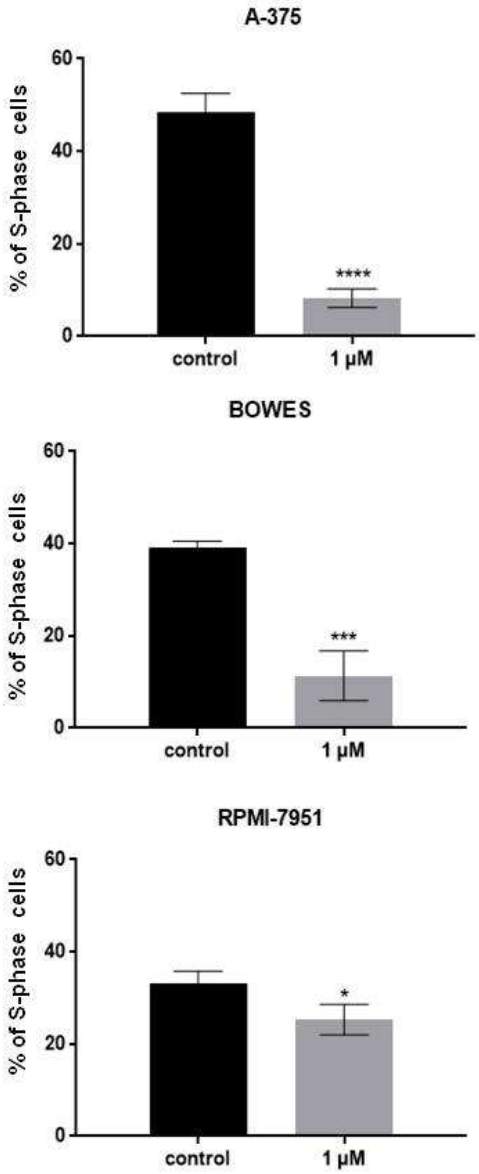

Figure 19 - Percentage of S-phase cells in A-375, BOWES and RPMI-7951 cells exposed to 1 µM flubendazole (FLU) during 24 hours as measured by EdU labelling assay. The data represent mean ± SD from three independent experiments. * $P < 0.05$, *** $P < 0.001$, **** $P < 0.0001$

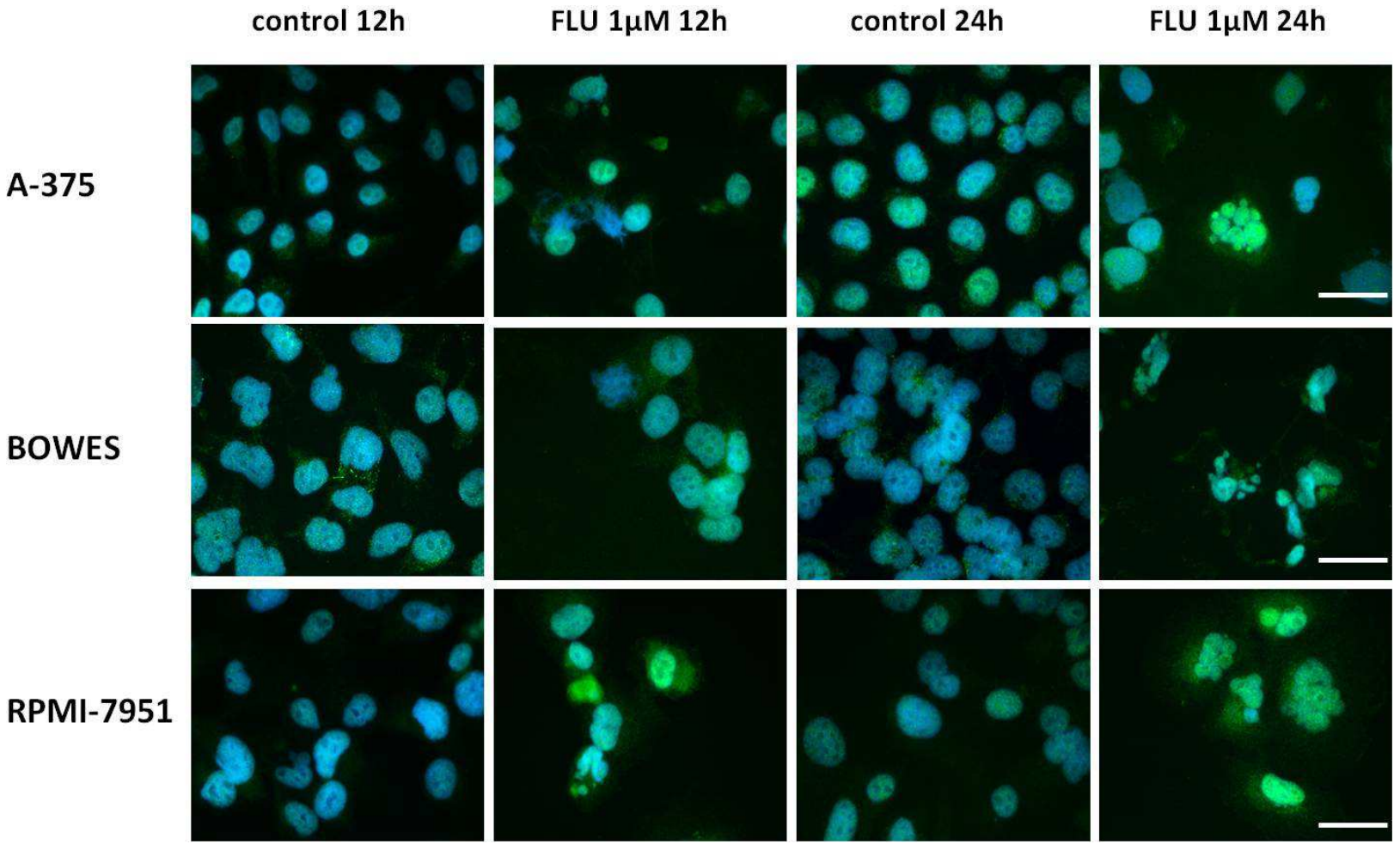

Figure 20 - Expression of p21 protein in A-375, BOWES and RPMI-7951 cells exposed to 1 µM flubendazole (FLU) during 12 hours and 24 hours as determined by immunofluorescent staining and cytometric analysis. Green – p21, Blue - nuclei. Fluorescence 400 x. Scale 10 µm.

7.5. Morphological changes in cells exposed to FLU

All used melanoma cell lines present differing cell size and morphology. These cells range from smaller (A-375) to larger (BOWES, RPMI-7951), mostly with prominent nuclei, multiple nucleoli and irregularly arranged and organized mitochondria and lysosomes (Fig. 21). Their growth is fast and population doubling is typically reached in 48-72 hours.

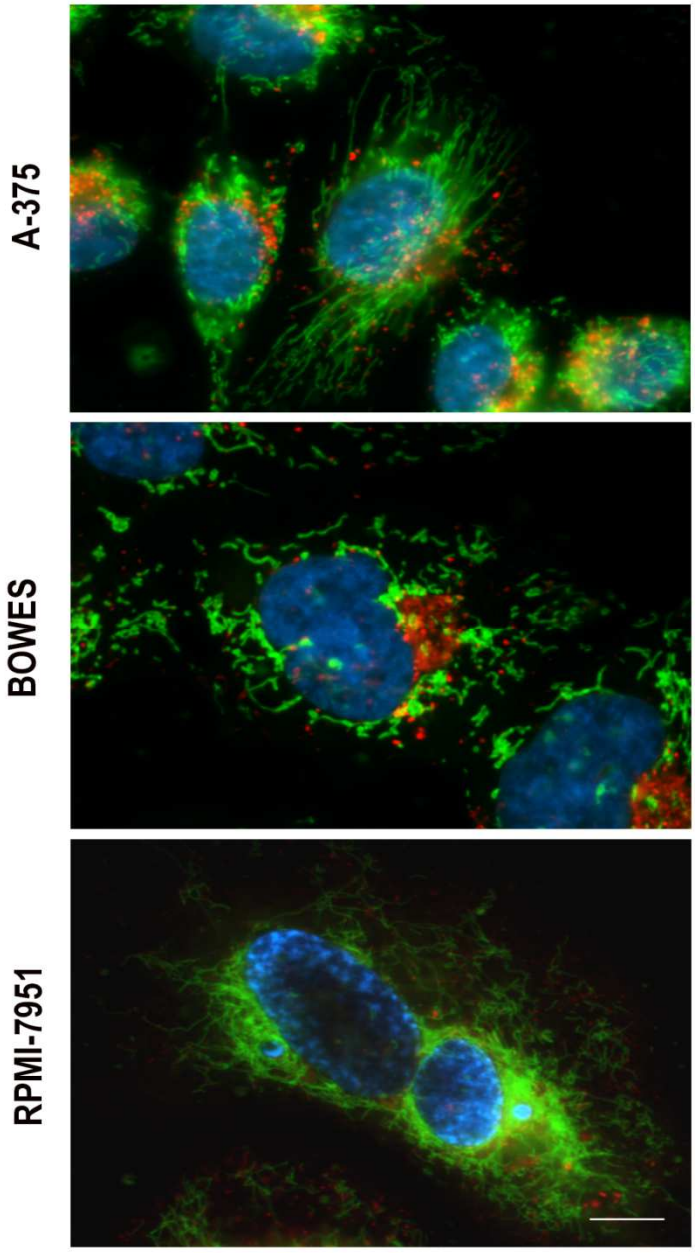

Figure 21 - Fluorescent labeling of mitochondria, lysosomes and nuclei in melanoma cell lines A-375, BOWES and RPMI-7951. Green-mitochondria, Red-lysosomes, Blue-nuclei. Fluorescence 600 x. Scale 5 µm.

Time-lapse morphological studies of 1 µM FLU exposed melanoma cells revealed that during first 12-24 hours of exposure cells grew and divided although less intensively than in controls. Approximately after 12 hours of FLU exposure, there appeared gradually larger cells with multiple nuclei, mainly in RPMI-7951 cultures. These multinuclear cells were not of the uniform dimensions and their nuclei differed in the size, shape and numbers too (Fig. 22). The status of multinucleated cells was confirmed with fluorescent staining using DNA-specific dye DAPI (Fig. 23). In addition, at later treatment interval of 24 hours, multinucleation reached further extent and some cells became giant in size.

Besides multinucleation, in A-375 and RPMI-7951 cells but very little in BOWES cells, the perinuclear vacuolization developed. As we could see in time-lapse records, these vacuolated cells persisted for another 12-24 hours and then lost their attachment became rounded and their membrane exhibited a series of rapidly bulging protrusions resembling blebs. Cell rounding and membrane blebbing lasted up to 1 hour and in most cases led to the final fragmentation of cell bodies into small elements. Alternatively, some rounded cells did not show membrane blebbing and quickly underwent fast cell demise without any marked morphological features (Fig. 24). The dynamics of the described changes in treated cells differed not only between individual cell lines but also among particular cells. Thus in A-375 and RPMI-7951 cell lines cell rounding, blebbing and fragmentation occurred asynchronously while in BOWES cell line cells appeared to follow individual steps more synchronously.

Another interesting phenomenon noted in the treated cells concerned the lysosomes. As shown in Fig. 21 melanoma cells lysosomes are mostly found concentrated around the nucleus, with some of them being scattered in the periphery too. Upon exposure to 1 µM FLU and along with changes in cell´s shape (cell rounding which occurred at about 24-48 hours of exposure) lysosomes grew more voluminous and became concentrated in the cell´s centre along with mitochondria (Fig. 25). Such lysosomal concentration and growth in volume was especially prominent in BOWES cells while in other two cell lines had a lower occurrence.

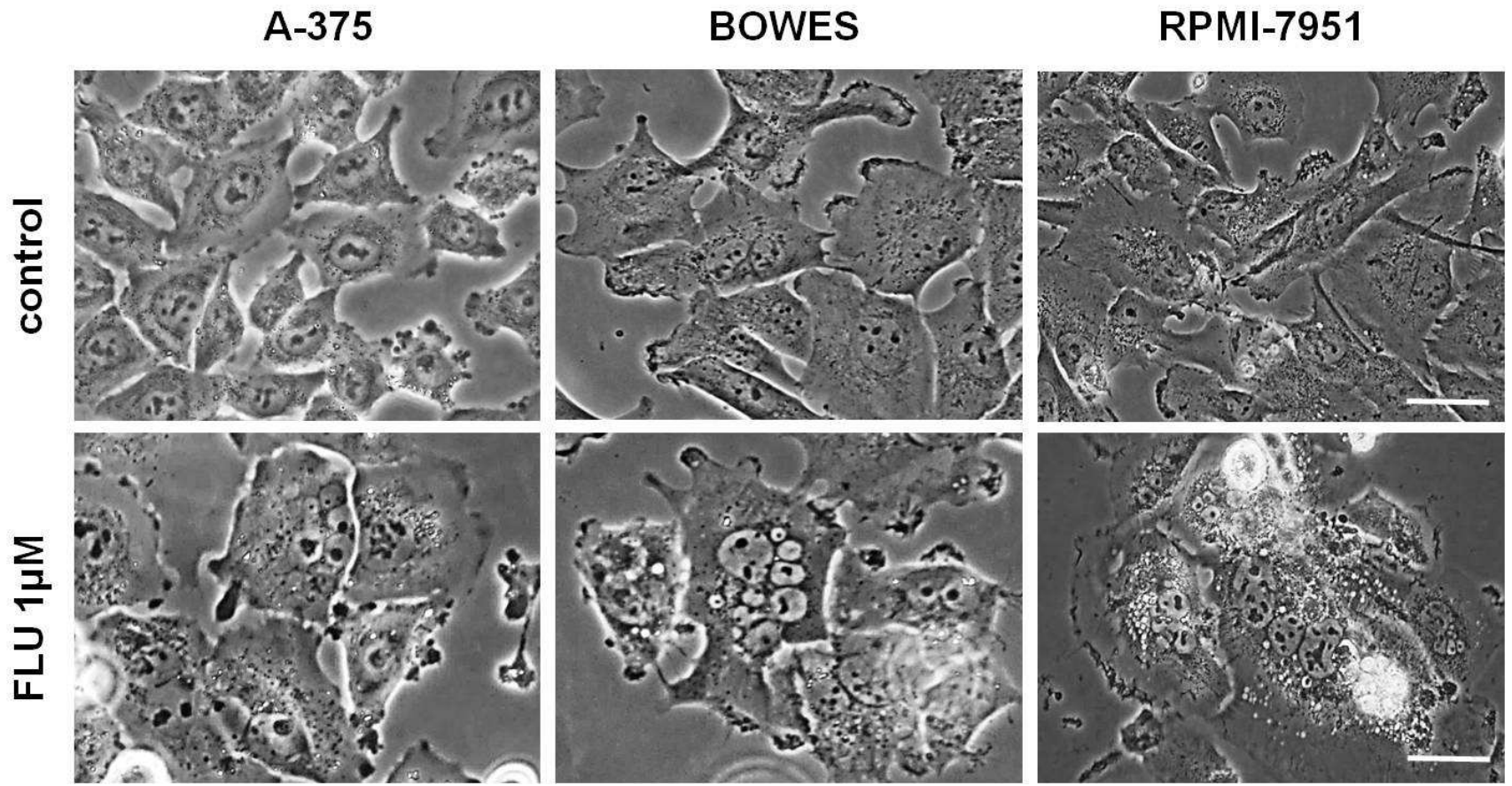

Figure 22 - Control cells and giant multinucleated cells after 12 hours treatment with 1 µM flubendazole (FLU). Phase contrast 600 x. Scale 25 µm.

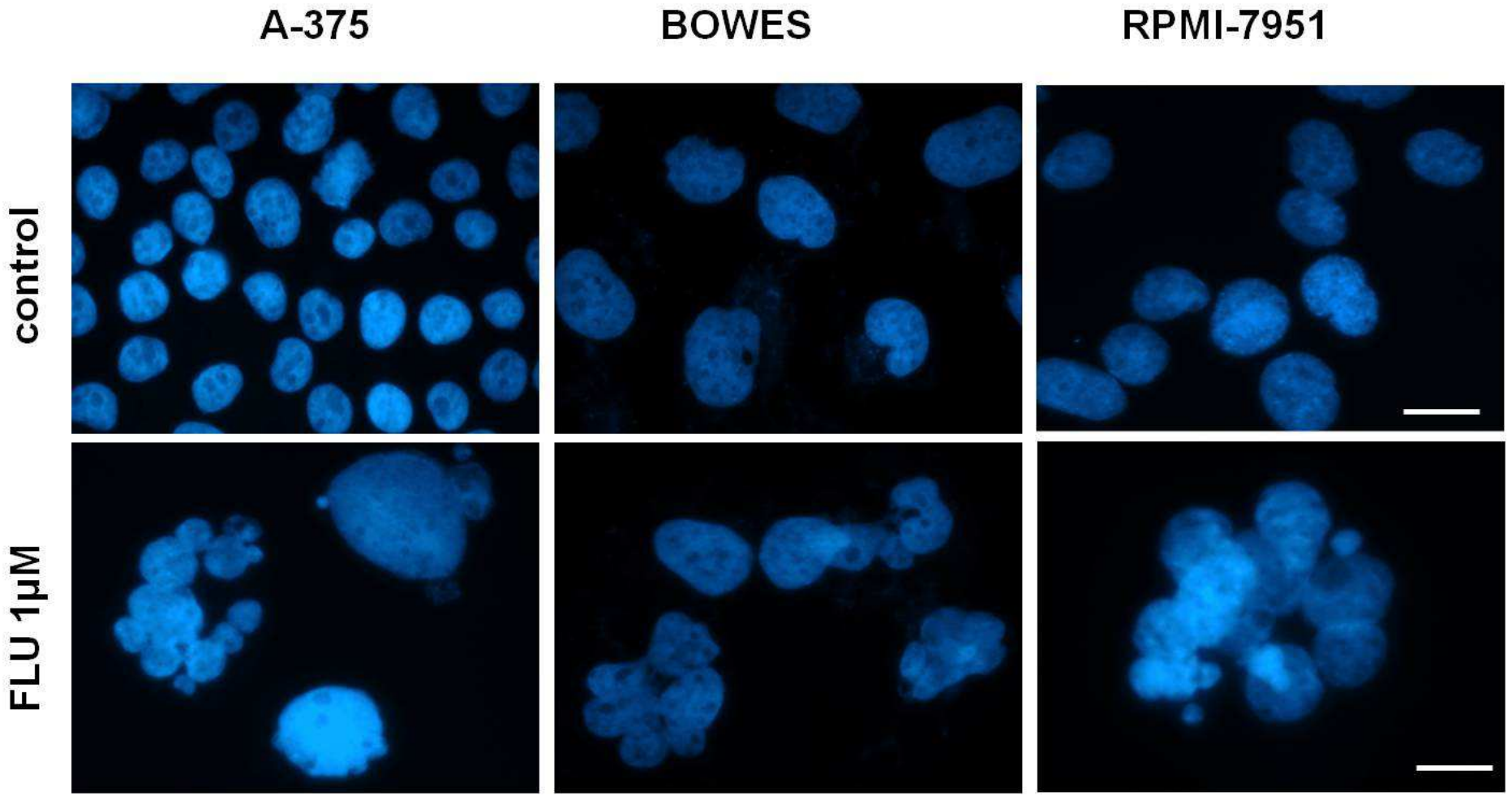

Figure 23 - Multinucleated cells after 12 hours treatment with 1 µM flubendazole (FLU). Fluorescent microscopy 600 x, scale 20 µm. Blue - nuclei.

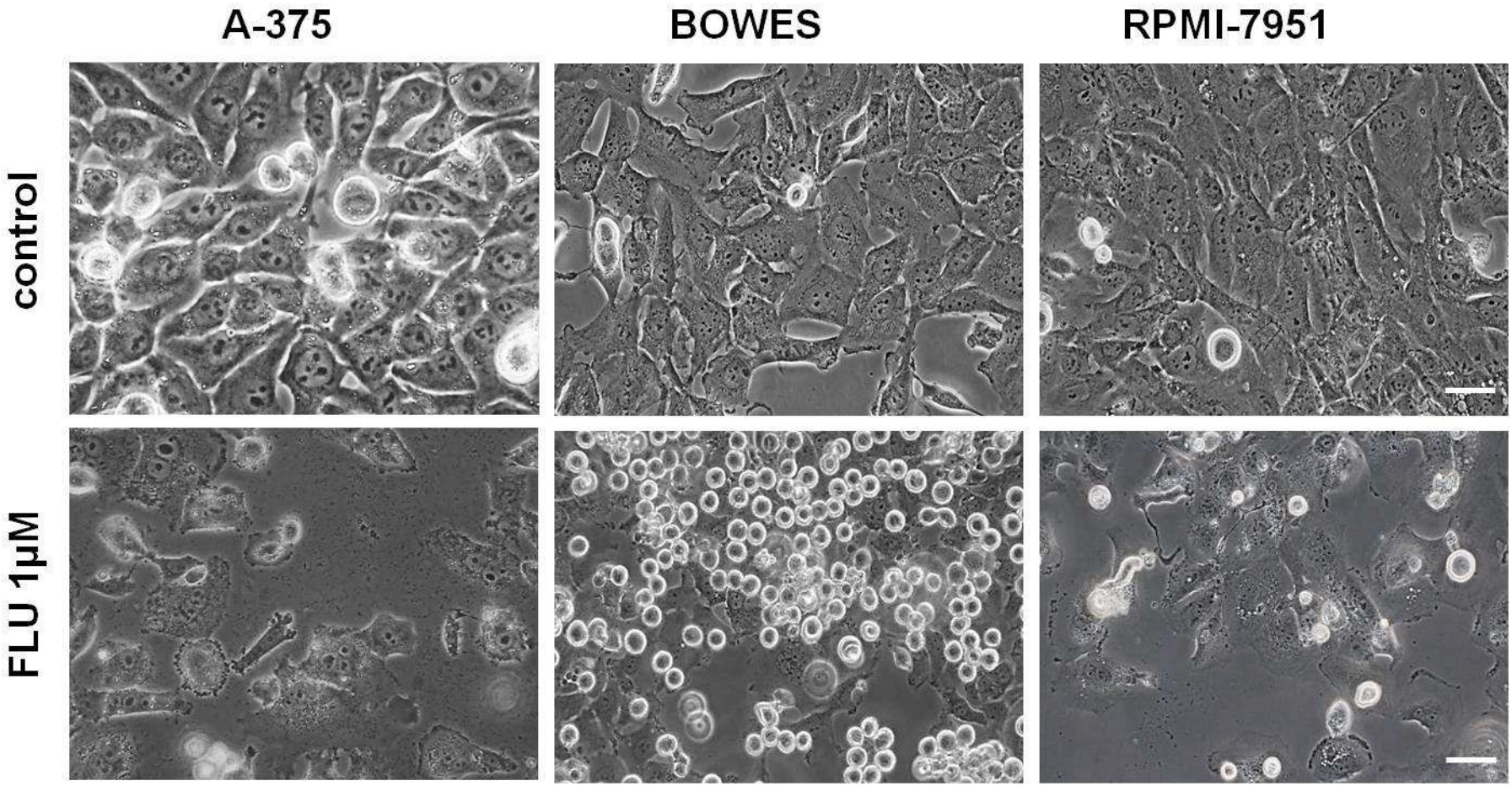

Figure 24 - Morphological changes in melanoma cell lines treated with 1 µM flubendazole (FLU) after 48 hours. Phase contrast 400 x. Scale 10 µm.

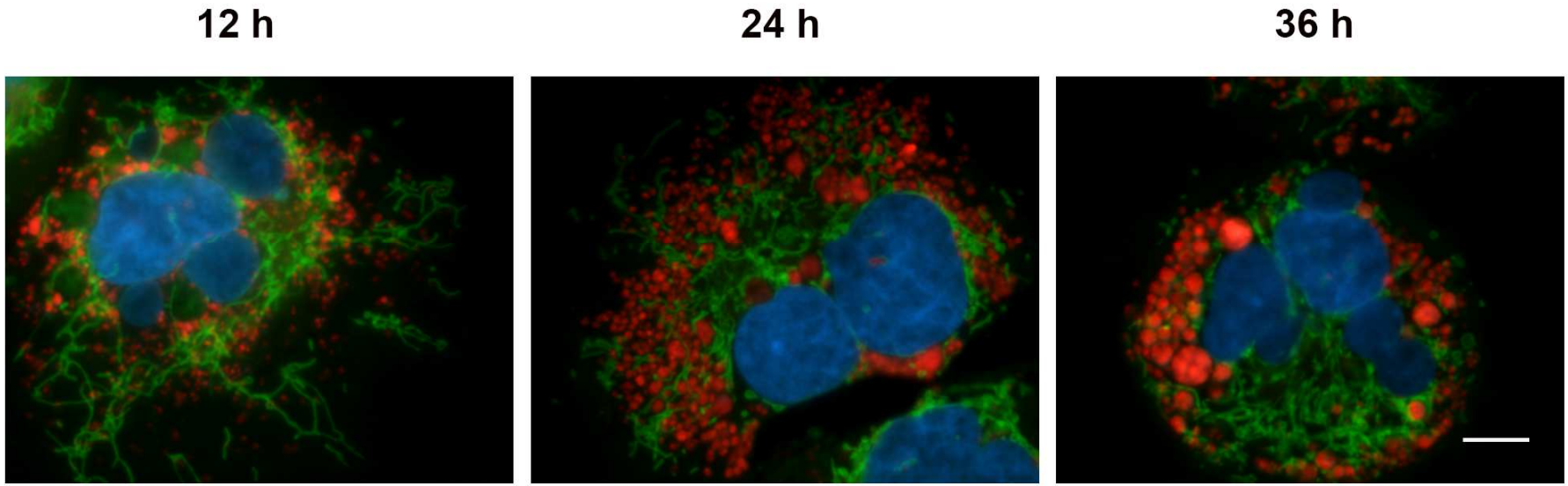

Figure 25 - Changes in lysosomal distribution and volume in BOWES melanoma cells treated with 1 µM flubendazole (FLU) during 36 hours. Green-mitochondria, Red-lysosomes, Blue-nuclei. Fluorescence 600 x. Scale 10 µm.

7.6. Effect of FLU on cytoskeleton

Our next efforts were aimed at investigation of the changes in the structure and arrangement of FLU main cellular target – cytoskeletal microtubules. In control cultures, microtubules of the interphase cells were typically organized from the single centrosome placed near the nucleus from which individual microtubule fibers extended to the periphery in a sheet-like pattern. During mitosis, microtubules rearranged into mitotic spindle attaching and separating chromosomes and upon cytokinesis connecting two arising cells by midbody.

Compared to control cultures, the number and the distribution of centrosomes in exposed cells after FLU treatment changed, which resulted in the presence of aberrant mitotic spindles and subsequent multipolar mitosis (Fig. 26). Also, microtubular network in interphase cells became disorganized too; microtubules were damaged and became compacted while losing their typical arrangement.

In addition to altered microtubular topography, some changes in actin filaments, namely their concentration in the subcortical regions of the cells, were noted too. Actin cytoskeleton is typically placed peripherally in melanocytes, in particular being positive in ruffling edges. In mitosing cells, actin forms a prominent ring surrounding mitotic spindle. In FLU exposed cells, actin distribution and or organization were not changed as severely as in the case of microtubules. Still, as mentioned before its accumulation and association with the cell membrane became more abundant (Fig. 26, 27).

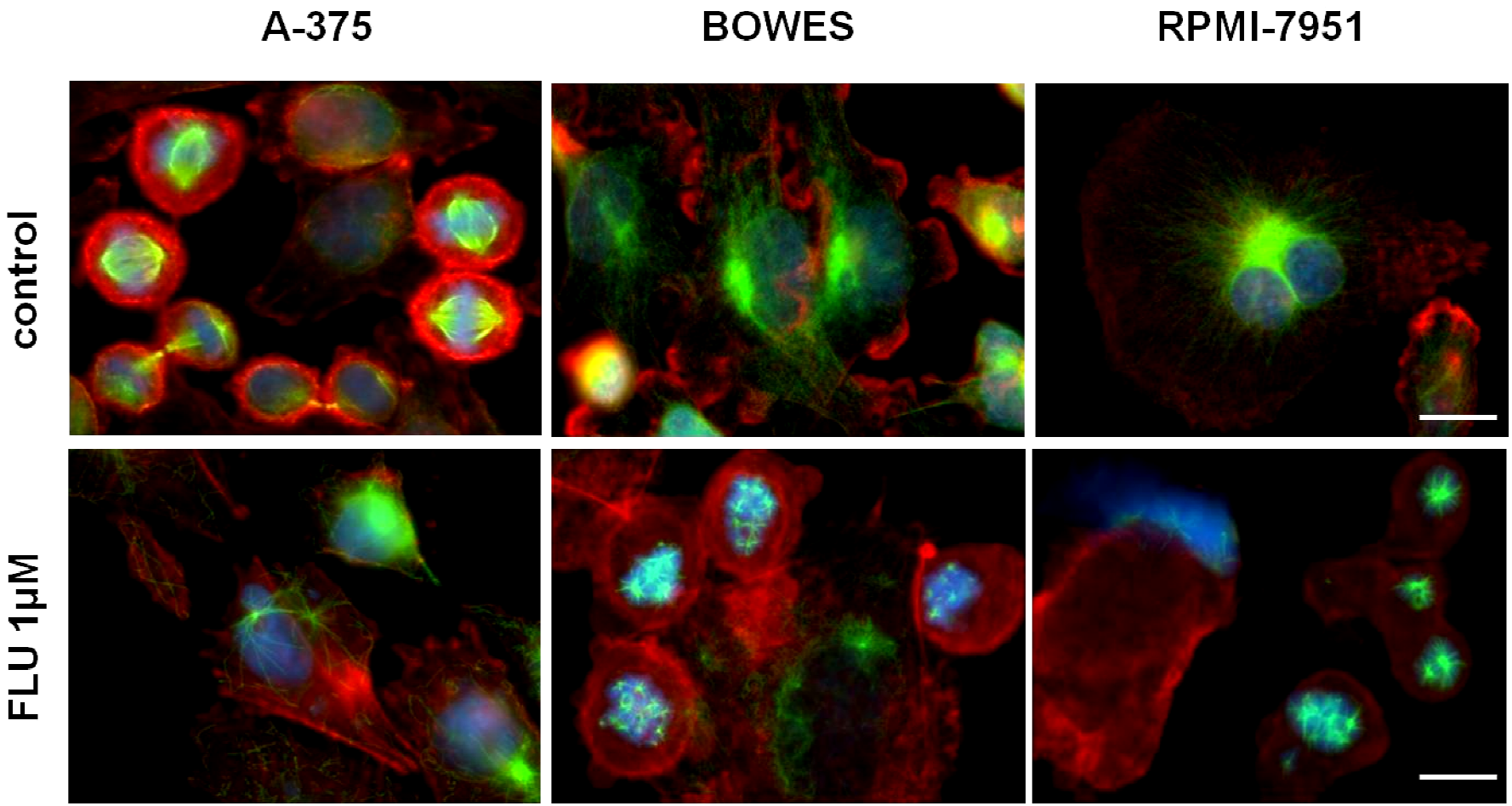

Figure 26 - Normal mitotic spindle in controls vs. aberrant multipolar spindle in 1 µM flubendazole (FLU) treated cells after 24 hours. Blue - nuclei, Green - α-tubulin, Red - β-actin. Fluorescence 600 x. Scale 10 µm.

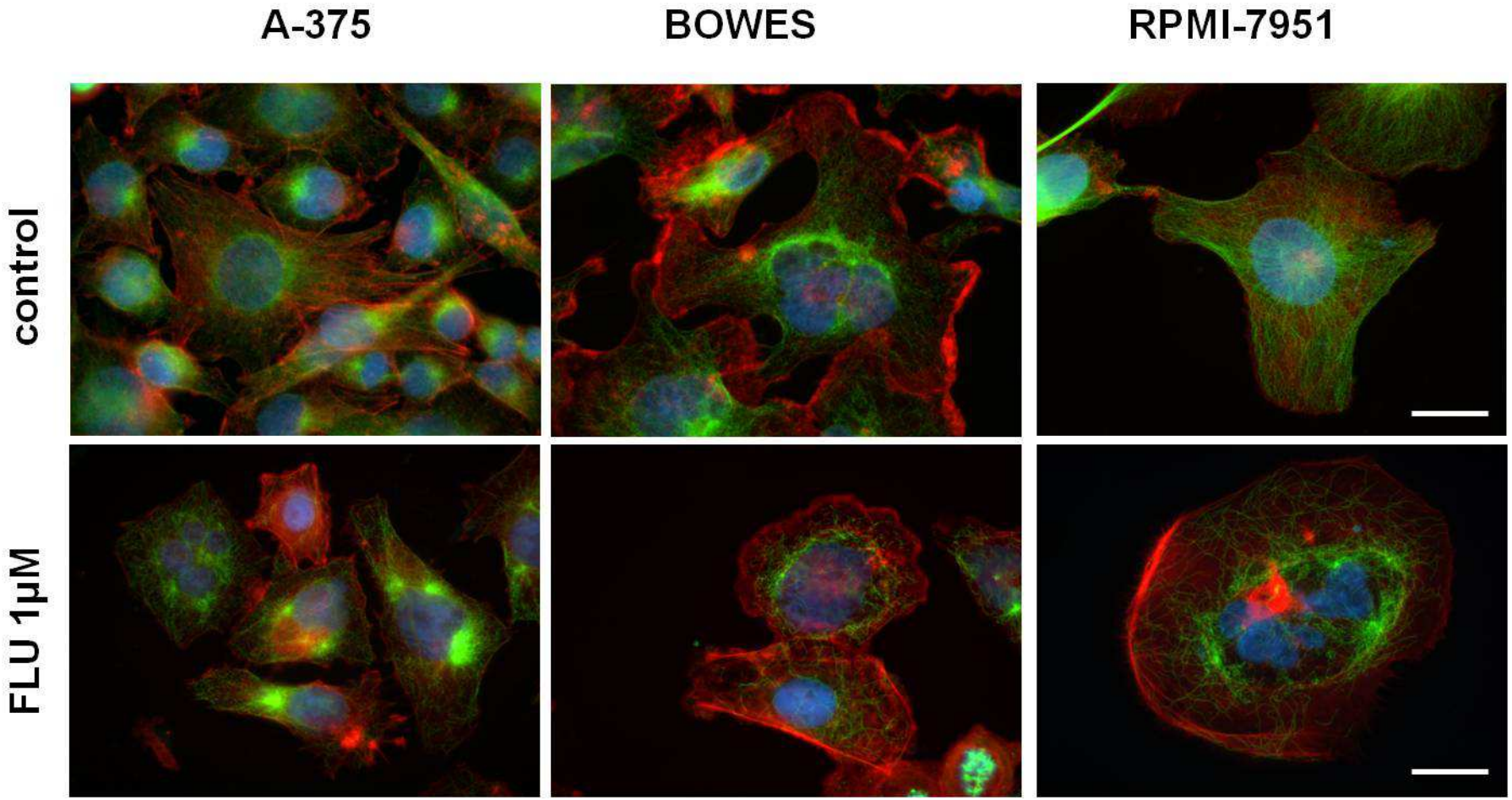

Figure 27 - Effect of 1 µM flubendazole (FLU) treatment on interphase cells cytoskeleton at 24 hours. Blue - nuclei, Green - α-tubulin, Red - β-actin. Fluorescence 600 x. Scale 10 µm.

7.7. Characteristics of FLU-induced cell death

As mentioned above in the section 7.5 melanoma cells exposed to 1 μM FLU underwent a series of morphological changes ranging from an early slight swelling to loss of adherence, formation of membrane protrusions – blebs and final rounding and fragmentation (Fig. 28). Still, not all exposed cells displayed all these steps, which, in addition, occurred in the context of multinucleation and cells enlargement. Despite the individual differences in these morphological changes and their timing the numbers of thus affected cells steadily grew in all tested cell lines where their proportions remained similar with exception of RPMI-7951 cells at 48 hours of treatment (Fig. 29). Along with changes in overall melanoma cells morphology and behaviour, some other typical markers of apoptotic cell death were present too. They included in particular the typical nuclear chromatin condensation and fragmentation (Fig. 30).

FLU-induced apoptosis was further confirmed by measurement of activity of selected caspases known to be typically associated with apoptosis and FLU-reported effects - caspase-2 and caspase-3/7. Time intervals of 12 hours, 24 hours and 48 hours were chosen for the measurement, using the standard luminescent assay. 1 μM FLU activated the caspases in all three cell lines but with a different time-course and efficiency. In A-375 cell line, caspase 2 and caspase 3/7 activities grew in a time-dependent manner, reaching their maxima at 48 hours of exposure. In BOWES cells the similar time dependency occurred too; however, the observed activities of individual caspases were lower and their dynamics varied too. Thus caspase-2 activity became significantly elevated at the end of the followed time interval (48 hours) whereas caspase-3/7 activity reached its peak already at 24 hours of exposure and persisted until the end of the experiment. In RPMI-7951 cell line, both caspases became least activated and their temporal organization differed too in comparison to the previous two cell lines. Caspase-2 reached the maximum activity at 24 hours of exposure of cells to FLU and then its activity decreased while caspase-3/7 activities remained the same once they became markedly elevated at 24 hours of exposure (Fig. 31).

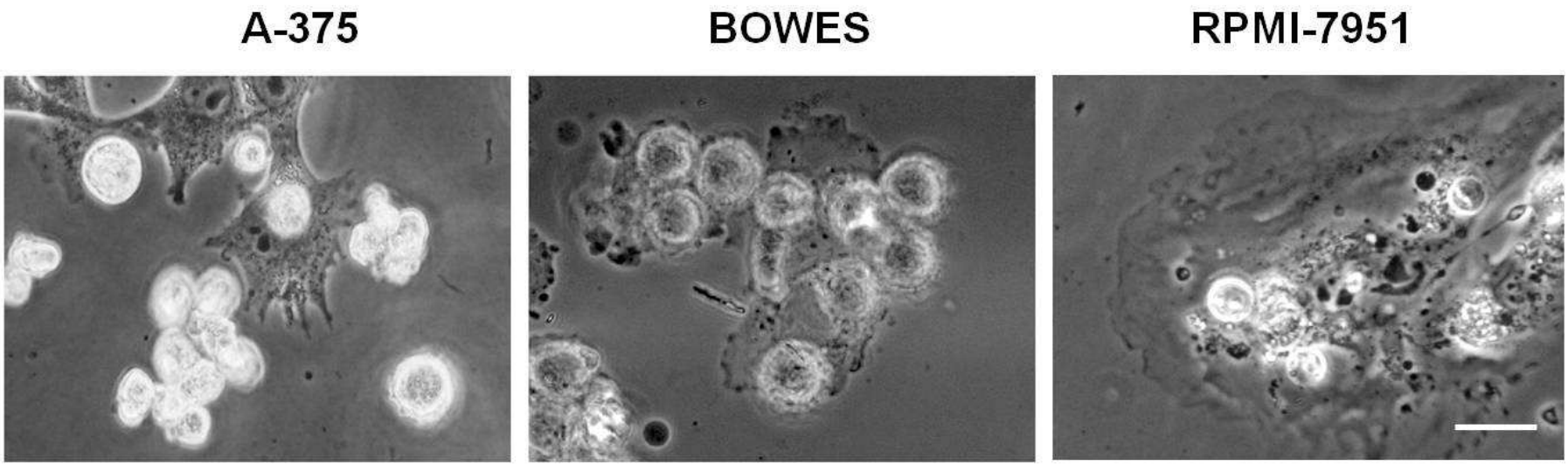

Figure 28 - Apoptotic morphology in A-375, BOWES and RPMI-7951 cells exposed to 1 µM flubendazole (FLU) at 36 hours. Phase contrast 400x. **S**cale 10 µm.

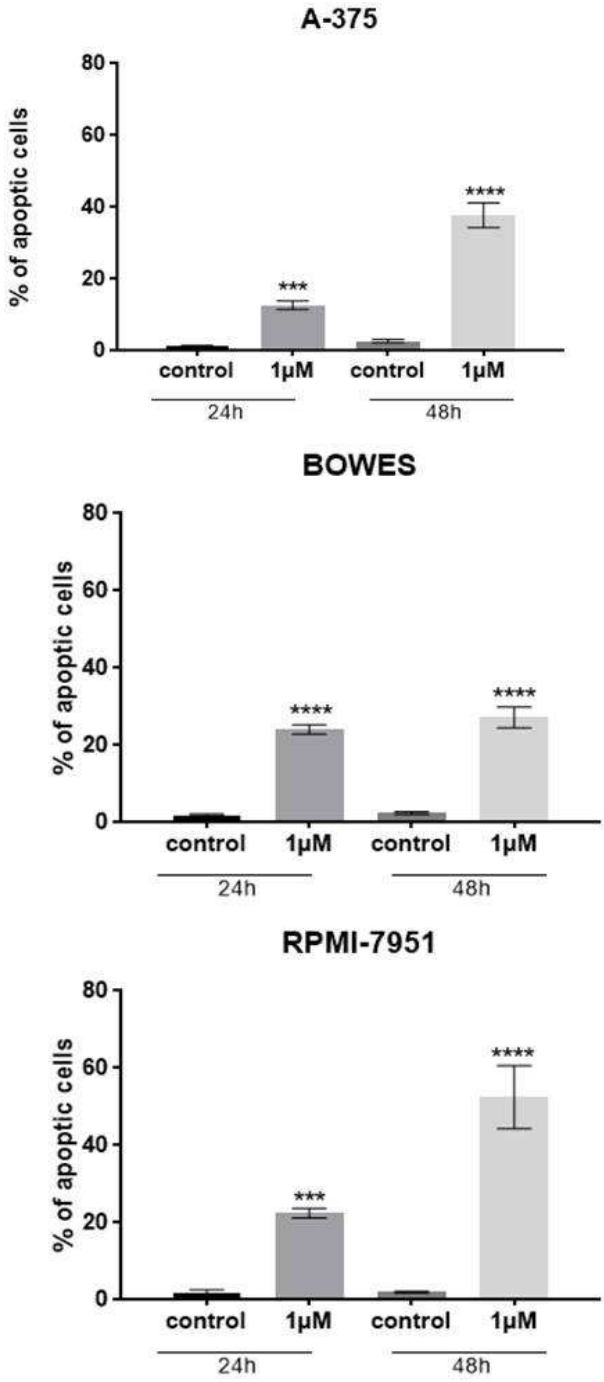

Figure 29 - Percentage of apoptotic cells after 24 hours and 48 hours treatment with 1 µM flubendazole (FLU) in A-375, BOWES and RPMI-7951 cells. The data represent the mean ± SD from three independent experiments. ** P < 0.01, *** P < 0.001, **** P < 0.0001

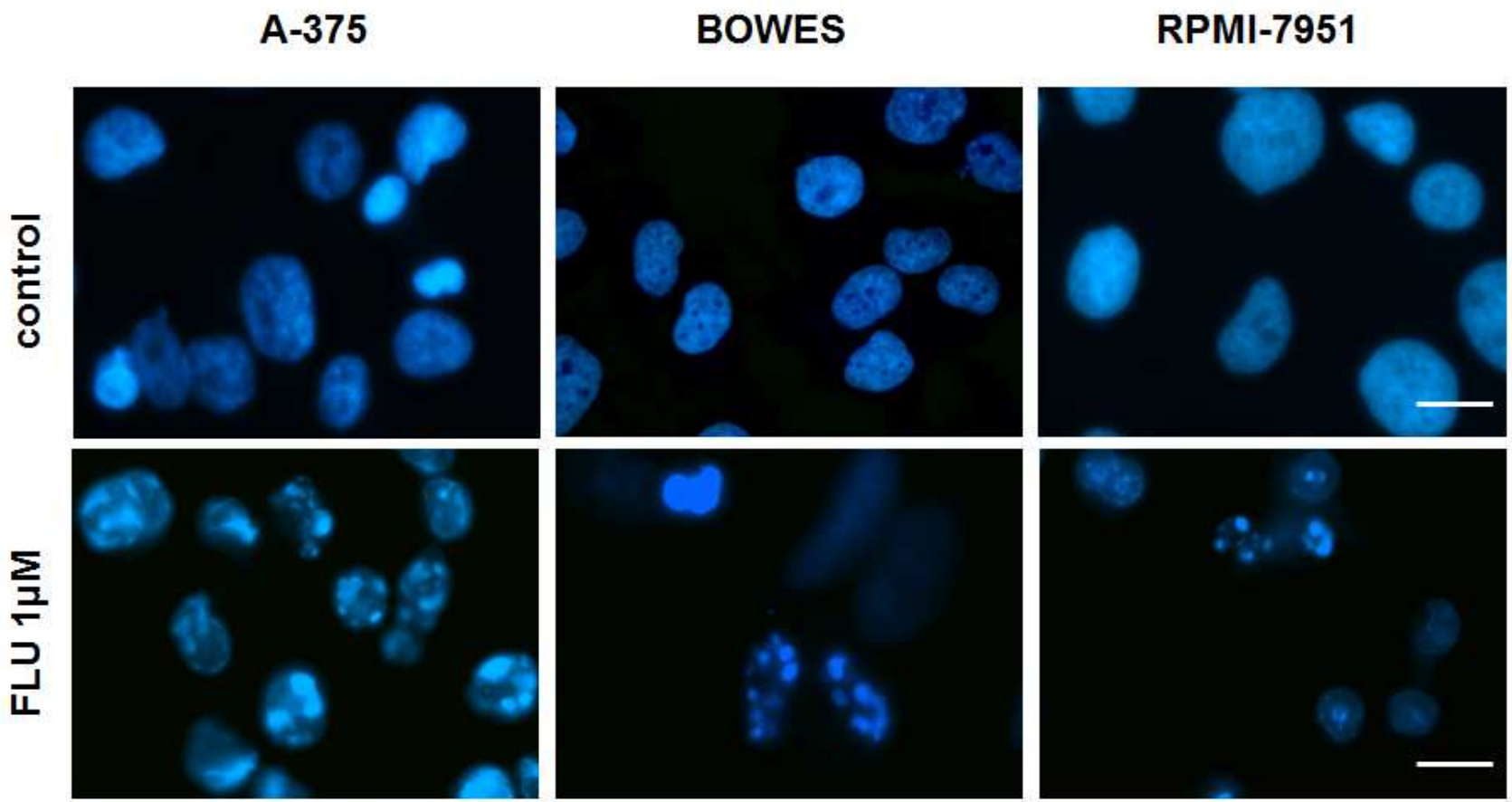

Figure 30 - Chromatin condensation in A-375, BOWES and RPMI-7951 cells exposed to 1 µM flubendazole (FLU) at 24 hours. Fluorescence 600 x. Scale 10 µm.

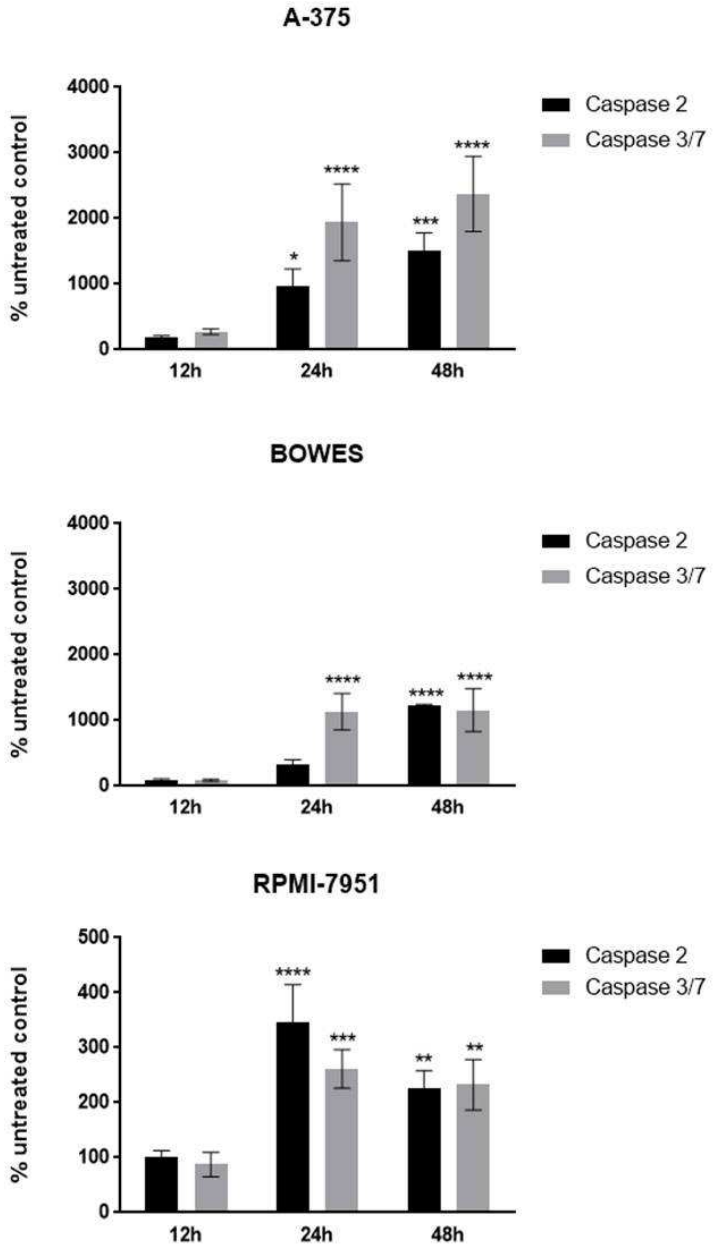

Figure 31 - Activity of caspase 2 and 3/7 in A-375, BOWES and RPMI-7951 cells treated with 1 µM flubendazole (FLU) during 48 hours. The data, presented as percentage control cells (=100 %), represent the mean ± SD from three independent experiments. * $P < 0.05$, ** $P < 0.01$, *** $P < 0.001$, **** $P < 0.0001$

7.8. Effect of FLU on *p53*-mediated proapoptotic signalling

Gene *p53* is a canonical regulator of so called intrinsic apoptotic pathways which act to activate cell demise by a series of biochemically controlled steps. Although *p53* is relatively rarely mutated in melanoma the chemoresistance of this type of malignancy is present in almost all of its advanced stages and may involve aberrant regulation of p53-dependent signalling. Since some benzimidazoles were reported to activate cell death in tumor cells via TP53-controlled signalling, experiments were carried out to determine whether 1 µM FLU-dependent cell death proceeds via this type of signalling too **(66)**. Immunoblotting analyses of *p53* expression as well as selected post-translation modifications of TP53 (namely at Ser-15 and Ser-46) in melanoma cells exposed to 1 µM FLU during 48 hours revealed a significant differences between tested melanoma cell lines. Thus on the one hand, a late (48 hours) marked increase in the TP53 protein abundance following the treatment with 1 µM FLU occurred in A-375 cells. Conversely, in BOWES cells no changes whether minor or significant were visible at all treatment intervals and stable TP53 protein levels were present. Moreover, in RPMI-7951 cells, we could not detect any TP53 protein expression in both controls and treated cells, which seems to confirm its already reported p53 null-status **(67)**. TP53 phosphorylations at Ser-15 and Ser-46 which are regarded as instrumental posttranslational modifications following DNA damage and activation of apoptosis were not significantly elevated in none of the tested melanoma cells. Similarly, changes in BAX and BCL-2 protein abundances in all treated melanoma cells were only marginal and not significant, suggesting that the classical TP53-BAX-BCL-2 axis was not markedly involved in FLU-induced cell death (Fig. 32).

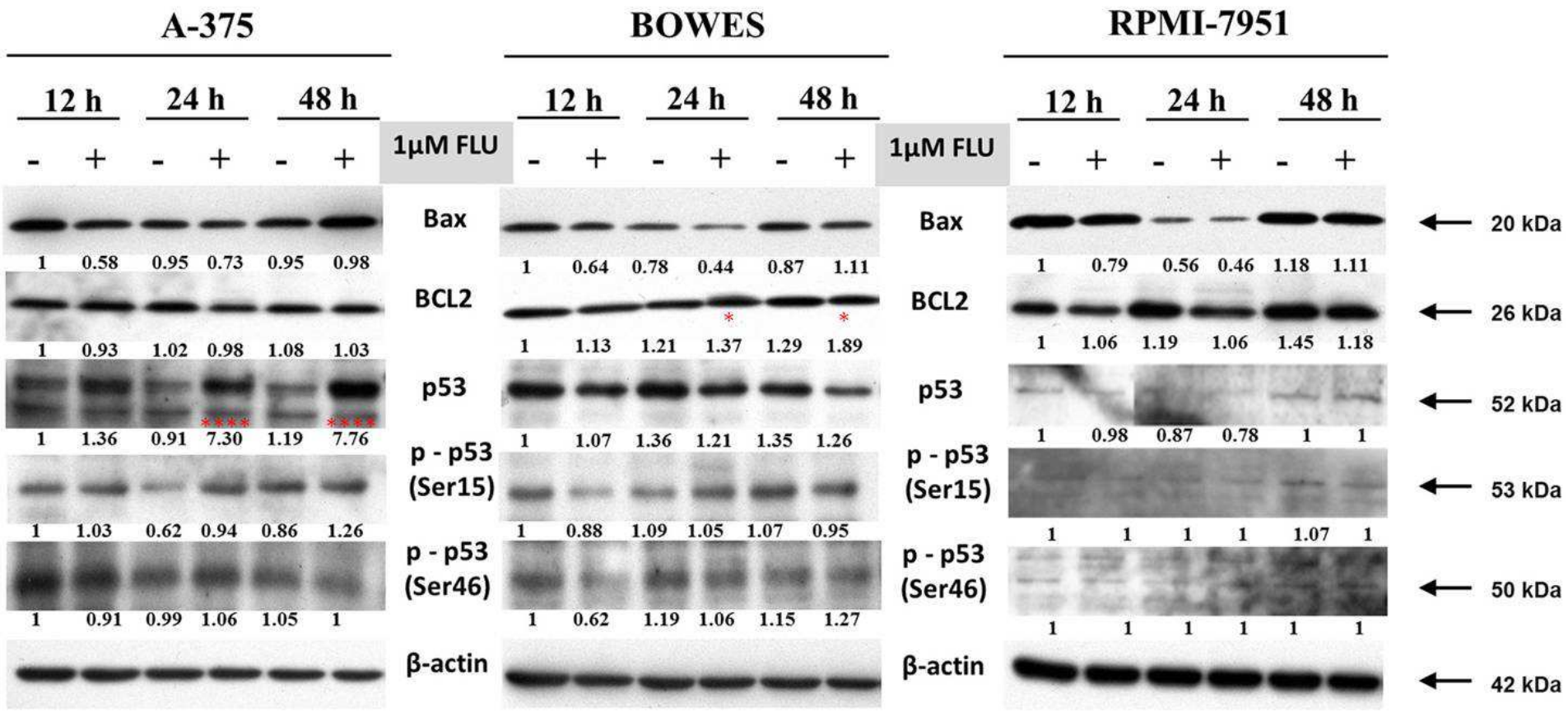

Figure 32 - The expression of proapoptotic proteins in melanoma cell lines A-375, BOWES and RPMI-7951 exposed to 1 µM flubendazole (FLU) as measured by immunoblotting analysis during 48 hours.
The data represent the mean ± SD from three independent experiments. * $P < 0.05$, **** $P < 0.0001$

7.9. Effect of FLU in primary melanoma explants

During 2013-2017 period, five cutaneous melanoma samples were obtained from Department of Plastic surgery, Faculty teaching hospital Hradec Králové. Samples were evaluated by a pathologist (Fig. 33) and then used for establishment of melanoma explant cultures in our laboratory, following the specified protocol. Resulting cultivations were in individual samples quite heterogeneous, containing varying proportions of mostly fibroblasts, melanocytes and other cells of oscillating size and behaviour (Fig. 34). With respect to such heterogeneity, both in terms of individual cell types and their characteristics, and taking into consideration cultivation success, one sample (M-170202) was selected to be used in pilot testing.

Cytotoxicity of FLU (range of original concentrations) in melanoma cells obtained from a primary explant isolated from a patient was evaluated using WST-1 assay. The results of this experiment showed a similar inhibitory effect of FLU compared to our employed melanoma cell lines A-375, BOWES and RPMI-7951, with 1 µM FLU being efficient already after 24 hours of exposure (Fig 35). Conversely, unlike in melanoma cell lines where this FLU concentration produced a consistently increasing inhibitory effect in time (the most significant inhibition occurred at 72 hours of exposure), in case of the investigated melanoma explant the FLU-dependent inhibition remained the same during 72 hours treatment. In addition, FLU IC_{50} value (as determined by GraphPad Prism Software) at 72 hours equalled to 1.42 µM; i.e. a markedly higher value than the one obtained from stabilized melanoma lines.

Cytometric studies of melanoma cells obtained from the melanoma explant showed that cells grew somewhat slower compared to the melanoma cell lines and typically varied in their size and appearance. When exposed to 1 µM FLU; i.e. sub IC_{50} dose, they responded by changing their internal organization which became often clumped into reticular-like formation. Furthermore, they developed larger vacuoles or vacuole-like structures and gradually displayed an altered adherence pattern. Conversely, unlike in thus treated melanoma cell lines, giant, multinucleated cells have not formed. During later treatment periods (24-48 hours), cells started to shrink, sometimes slowly or rapidly extending their cytoplasmic membranes (Fig. 36). Subsequently observed cell demise was generally much less homogeneous then in the treated melanoma cell lines and comprised at least three distinct patterns – 1) individual cell shrinkage accompanied by plasma membrane undulation, 2) collective rapid shrinkage without any marked cell

membrane activity and 3) internal coarsening and fragmentation followed by cells implosion.

Sample No.	*Gender*	*Age (years)*	*Tumor type*	*Classification*			
				Breslow	*Clark*	*MKNO*	*TNM*
M - 130328	Male	53	Nodular malignant skin melanoma	9 mm	II	8721/33	pT4b, pNX, pMX
M - 141022	Female	61	Lentigo maligna skin melanoma	0.25 mm	III	8742/32	pT1a
M - 150325	Male	52	Nodular malignant skin melanoma	2.2 mm	IV	8721/32	pT3b, pNX, pMX
M - 160121	Female	72	Nodular malignant skin melanoma	1,9 mm	III	8721/33	pT2b, pNX, pMX
M - 170202	Male	84	Nodular malignant skin melanoma	4 mm	IV	8721/33	pT3a, pNX, pMX

Figure 33 – Basic histopathological characteristics of obtained human melanoma samples as provided by The Fingerland Department of pathology Faculty teaching hospital Hradec Králové.

T-size and extend of primary tumor *

NX - cancer in nearby lymph nodes cannot be measured *

MX - metastatis cannot be measured *

(*Staging. *National Cancer Institute* [online]. Available from: https://www.cancer.gov/about-cancer/diagnosis-staging/staging)

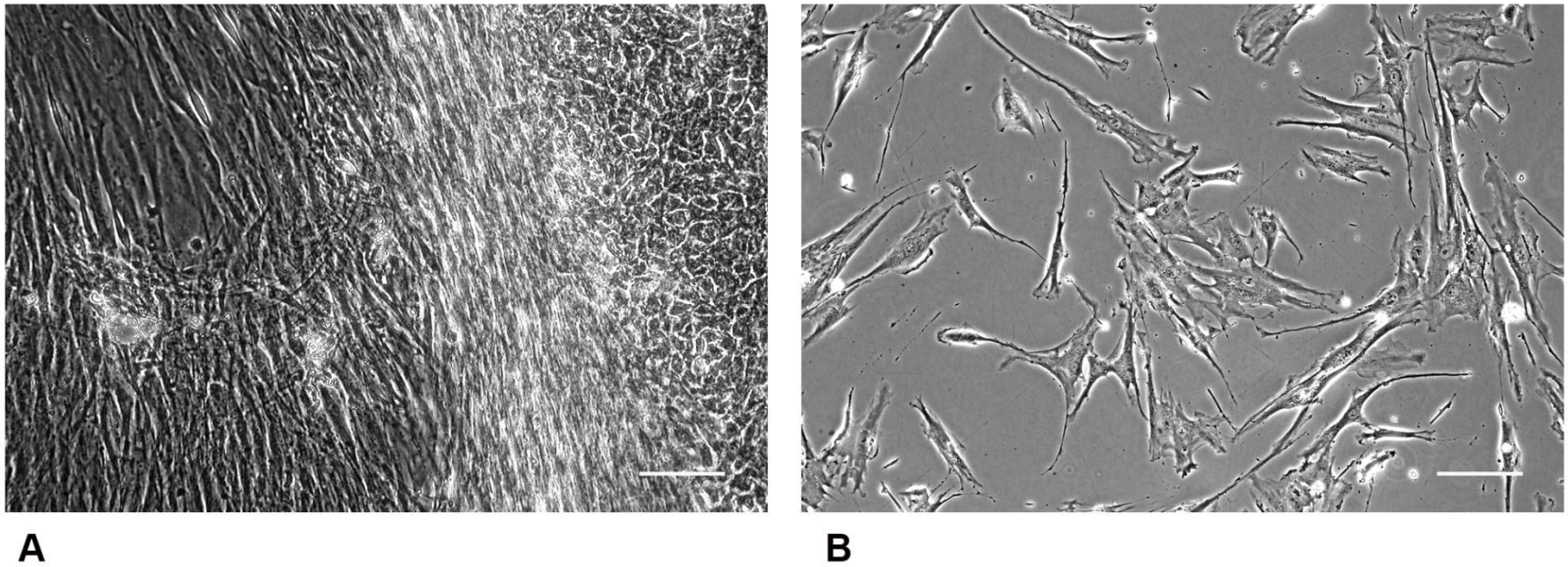

Figure 34 – (A) Melanoma explant in culture. Phase contrast 200x. Scale 10 µm. **(B) Explant-derived melanoma cells in culture.** Phase contrast 400x. Scale 10 µm.

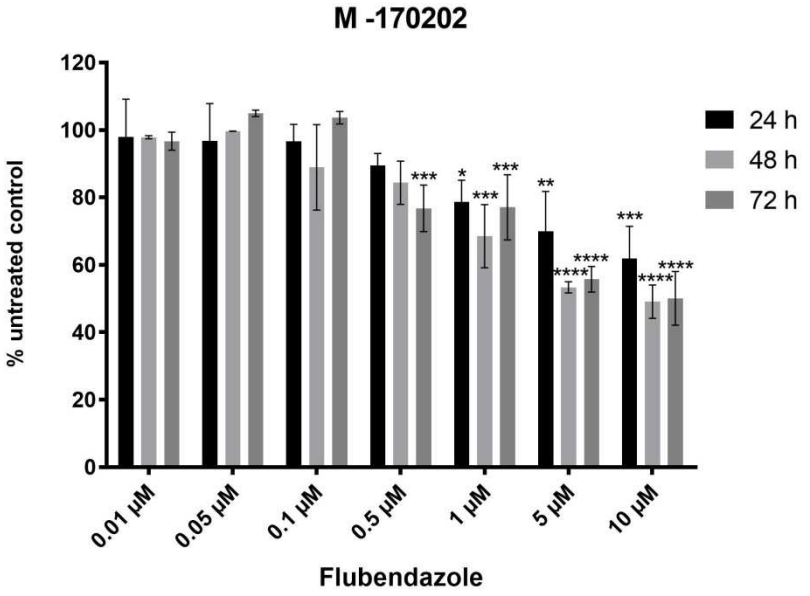

Figure 35 - Proliferation of M-170202 treated with flubendazole (FLU) at a concentration range 0.01 - 10 µM using WST-1 assay. The data represent mean ± SD from three independent experiments. * P < 0.05, ** P < 0.01, *** P < 0.001, **** P < 0.0001

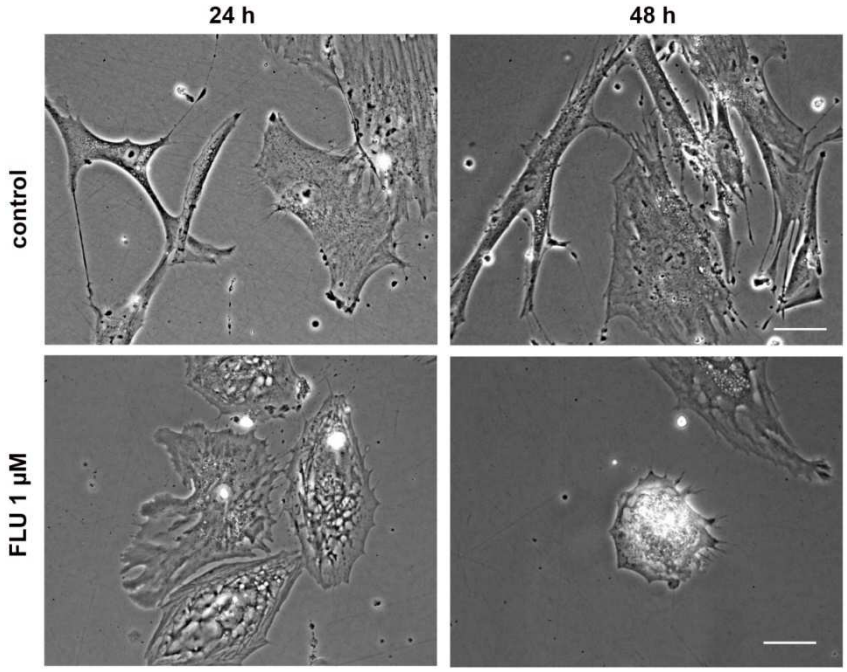

Figure 36 - Morphological changes in explant-derived melanoma cells treated with 1 µM flubendazole (FLU) after 48 hours. Phase contrast 600 x. Scale 5 µm.

8. DISCUSION

Malignant melanoma represents a relatively rare but very dangerous form of skin malignancy which is at its advanced stage characterized by an aggressive growth with the high propensity for metastatic spread and chemoresistance. Accordingly, no effective cytotostatic treatment of advanced malignant melanoma is currently available and new targeted therapies show only limited clinical efficiency upon life-long burden **(33).** Thus continuing studies of melanoma biology are aimed at identification of novel putative targets in malignant melanocytes, which could be used for development of effective treatments. Alternatively, via revisiting already established therapeutical concepts the scientific efforts endeavour to find their new applications for the future treatment of this malignancy **(45)**.

One of traditional and yet novel targets in malignant cells is cytoskeleton, and namely microtubules. Microtubules are the major cytoskeletal components in all eukaryotic cells where they play a substantial role in various processes such as mitosis, intracellular transport and signalling or maintenance of cell shape and polarity **(68)**. In particular, during cell division, microtubules form the mitotic spindle which has become an essential target for the chemotherapeutic approach in a wide spectrum of malignancies. The effectiveness of microtubule-targeting drugs has been validated by the successful use of several vinca alkaloids and taxanes for the treatment of several human cancers. Their clinical success has prompted a worldwide search for compounds with similar mechanisms of action but improved characteristics, mainly due to the prevailing existence of toxic side-effects and developed chemoresistance **(69, 70)**.

At the end of the last century, first experimental studies were published demonstrating cytotoxicity of selected benzimidazole carbamates (i.e. albendazole and mebendazole) in several cancer models **(57, 66, 71-74)**. Although originally approved for treatment against parasitic worms both in humans as well as in animals, their selective targeting of microtubules quickly prompted scientific inquiry into their possible utility as antiproliferative agents **(57, 66, 71-74)**.

The first report on antitumor activity of FLU concerned its effects against leukaemia and myeloma cells where low FLU concentrations induced mitotic catastrophe and cell death in malignant cells and delayed tumor growth *in vivo*. Still more importantly, in cells resistant to vinblastine due to overexpression of P-glycoprotein sensitivity to FLU was retained **(75)**. In the subsequent studies carried out on several breast cancer cell

lines (MDA-MB-231, BT-549, SK-BR-3 and MCF-7) and panels of colon cancer as well as neuroblastoma cell lines, FLU displayed its broad suppressive activity via diverse mechanisms **(76, 77)**.

Based on these previously published experiences with FLU, in our present work we wanted to investigate the potential cytotoxic activity of FLU in an *in vitro* model of human skin melanoma using firstly several established melanoma cell lines with diverse molecular phenotypes. The employed cytotoxicity assays measuring distinct endpoints showed that predictably FLU inhibited cell growth and proliferation of all used melanoma cell lines, however, with a time and concentration dependence. In addition, the existence of varying sensitivity of exposed cells (as indicated by particular achieved IC_{50} values) most probably reflected an inherent heterogeneity of response among individual cell lines which was already demonstrated with other benzimidazole derivatives and melanoma cell lines **(72)**. Based on these initial experiments, we chose 1 µM concentration of FLU for further testing in melanoma cells while verifying its effect on normal human skin melanocytes. Our results indicate that FLU had cytostatic effect in these cells as judged from their rapid morphological changes (i.e. flattening and spreading), slowed growth and at least initially increased cell demise. On the other hand, these adverse changes lessened over the later time periods (48 hours and onward) and during this time interval some exposed melanocytes resumed their dynamics and proliferation. Thus it would seem that the employed 1 µM FLU is in this model of normal skin cells sufficiently tolerated. Nevertheless, at the same time one must be aware that this "tolerance" might be due to the rather special status of melanocytes. Melanocytes are responsible for melanin synthesis in the skin and as such they are highly resistant against environmental stresses and apoptosis, namely one induced by UV. Their tolerance to FLU therefore needs to be confirmed and compared with other skin cells (fibroblasts or keratinocytes) to verify whether normal skin would not be more seriously affected by this type of compound.

To further identify the mechanisms of FLU cytotoxicity in tested melanoma cell lines, we next carried out cell cycle analysis, which revealed that in treated cell populations FLU significantly increased G2/M fraction cells upon corresponding decrease of the G1 phase and S phase cells. This G2/M phase arrest seems to be characteristic of many benzimidazole carbamate actions in tumor cells as it was also observed in albendazole-treated liver cancer and colon cancer cells and FLU-exposed colon cancer cells **(56, 66)**.

As well as suffering the specific cell cycle arrest, FLU-treated melanoma cells further underwent a series of morphological changes which differed in their spatiotemporal organization and included: 1) early intracellular vacuolization, cell enlargement, coarsening of the cytoplasm and multinucleation and 2) later loss of adherence, cell rounding, cell volume shrinkage and membrane blebbing. Of all present changes, intracellular vacuolization was noted only sporadically in some exposed cells of BOWES cell line only. Specific staining subsequently revealed that vacuoles were accumulating and enlarged lysosomes concentrating around cell nuclei together with clumped mitochondria, owing most probably to the collapsing microtubular network. Whether thus changed lysosomal compartment lost its integrity and contributed to the lysosomal cell death of individual cells was not further verified. Still, induced vacuolar stress leading to autophagy via ROS or other more specific mechanisms was already reported in MDA-MB-231 breast cancer cell line treated with FLU **(55)**. Furthermore, a very recent report brought evidence of autophagy in HCT-116 colon cancer cells in which mitotic catastrophe was induced by doxorubicin. Authors concluded that mitotic catastrophe induction leads firstly to autophagy with subsequent apoptosis and the balanced interplay between these two processes is determined by mitotic catastrophe intensity **(61)**. It seems, however, that this form of cell demise was only incidental upon current treatment conditions and thus its role was minor. Conversely, emergence of giant multinucleated cells was nearly universal in our model and clearly associated with the primary target of FLU in exposed cells – microtubules. FLU modifies microtubule structure and inhibits tubulin polymerization by interacting with a site on β-tubulin similar to colchicine but distinct from vinca alcaloids **(75)**. Accordingly, in our model melanoma lines FLU altered microtubular cytoskeleton in dividing cells with an increased presence of aberrant multipolar spindles and abnormal mitosis. In addition, in interphase cells FLU produced visible alterations in microtubular topography too. Together these results suggested the presence and activation of the process called mitotic catastrophe.

Mitotic catastrophe was historically first described as the process of microtubule disintegration **(78)**. Nowadays, this term often denotes a mechanism of a delayed cell death associated with mitosis. On the other hand, several reports argue for an alternative view of mitotic catastrophe, which is presented as a process resulting from aberrant mitosis and leading to cell death – apoptosis or necrosis **(79, 58)**. Since mitotic catastrophe may be induced not only by mitotic/spindle inhibitors but also by DNA

damaging agents, inhibited mitotic proteins or via replication fork stress, it shows a number of morphological and biochemical characteristics **(58)**. In our FLU-treated melanoma cells, several of these characteristics were present such as persistent G2/M phase block, the overexpression of cell cycle inhibitor p21, multinucleation of cells and elevated activity of caspase-2, which clearly demonstrates the activation of this process. Interestingly, mitotic catastrophe has also been described to be accompanied by chromatin condensation, mitochondrial release of proapoptotic cytochrome c and apoptosis inducing factor (AIF), caspase activation and DNA degradation **(79)**, i.e. features typical of apoptosis implying a tight linkage between both processes. Our obtained results confirm this linkage since FLU-exposed melanoma cells ultimately showed typical apoptotic morphologies with membrane blebbing and nuclear chromatin condensation. To this effect, we have also verified apoptosis by detecting increased activity of caspase-3/7.

Mitotic arrest and catastrophe are strongly associated with apoptosis but the exact molecular mechanisms of this association remain unclear. Two proposed schemes include both *p53*-independent and *p53*-dependent events despite the fact that multiple lines of evidence argue for the important role of *p53* **(80)**. Despite already reported FLU capacity to induce *p53*-dependent apoptosis in neuroblastoma cells **(77)**, our data obtained from treated melanoma cells argue differently. FLU induced increased expression of TP53 in A-375 cell line only. Moreover, concomitant TP53 phosphorylation concerned Ser-15 (i.e. modification enhancing TP53 accumulation) but not Ser-48 (i.e. modification regulating the ability of this protein to induce apoptosis), suggesting the non-direct involvement of this protein in induced apoptosis **(81)**. Further to this, elevated activity of caspase-2 in our exposed cells hint at *p53*-independent apoptosis since this conserved initiator caspase has been previously implicated both in mitotic cell death as well as mitotic catastrophe, via MOMP-dependent and *p53*-independent process **(82)**.

The activity of the BCL-2 protein family is a key determinant of fate following mitotic catastrophe **(83-87)**. The family consists of multidomain prosurvival proteins (BCL-2, BCL-$_{XL}$, BCL-$_{W}$, MCL1, A1, and BCL-B) and multidomain proapoptotic effector proteins (BAX, BAK, and BOK) as well as BH3-only proteins (BIM, PUMA, BAD, NOXA, BIK, HRK, BMF, and tBID) **(87)**. The multidomain members of the family (the prosurvival proteins and the effectors BAK, BAX, and BOK) contain four BCL-2 homology regions (BH1–BH4), whereas the BH3-only proteins contain only

a BH3 domain, which is important in mediating their interaction with the multidomain members. Out of them, BCL-2 protein is widely expressed in human melanoma and has been linked to melanoma chemoresistance through its antiapoptotic function **(88)**. It has been reported that mebendazole, a benzimidazole derivate related to FLU, inhibits melanoma cellular proliferation through a BCL-2–mediated cellular response to microtubular damage **(72)**. Furthermore, mebendazole-mediated inhibition of melanoma growth *in vivo* is accompanied by phosphorylation of BCL-2 and decreased levels of X-linked inhibitor of apoptosis (XIAP) via mitochondrial SMAC/DIABLO **(81, 89)**. Contrary to these findings, neither BCL-2 nor BAX proteins showed elevated abundances in our FLU-treated melanoma cells, implying their negligible role in the present apoptotic process. The lack of significant involvement of TP53 and selected BCL-2 family proteins in this setting prompts further questions concerning the exact mechanism of apoptosis activation. For instance, some of the relevant points to ask are: (a) Are other BCL-2 protein family members involved and to which extent? (b) Do mitochondria play direct role? And if so which one? (c) What is the mechanism of caspase-2 activation? (d) How universal is mitotic catastrophe-apoptosis induced by FLU in melanoma types? These and other questions will no doubt need to be addressed in future to provide mechanistical basis for further preclinical and clinical testing of FLU in melanoma.

To provide some initial information on this matter, the above-mentioned ability of FLU to inhibit growth and proliferation of melanoma cells while inducing their mitotic catastrophe and apoptosis was tested in cells derived from a melanoma explant culture established from human melanoma excisions. As explained in the Results section, all five samples of malignant melanoma were of differing histopathological grade and comprised several cell types at various initial proportions and biological properties. Their detailed characterization and sorting was not a primary objective of the present work, however, and thus resulting primary cultivations contained a mix of cellular phenotypes which in our opinion reflects more accurately on real tumor composition. Based on the growth and cultivation characteristics of cells of all samples one was ultimately chosen for pilot testing. These cells were firstly maintained upon standard laboratory conditions to verify their growth and proliferative characteristics and then exposed to a range of FLU concentrations to determine its effects. Similarly to stabilized melanoma cell lines, FLU induced time and concentration-dependent inhibition of growth and proliferation of melanoma cells, however, its potency was

lower as also judged from higher IC_{50} value. In addition, time-lapse morphological studies of treated melanoma cells revealed an entirely different FLU effect; i.e. cells have practically failed to form giant multinucleated structures, changing instead from inside out and forming a reticular-like structure in their cytoplasm followed by internal implosion. The presence of classical, morphologically distinct apoptosis was very low and cells often quickly shrank, resembling necrosis-like bodies. These observations are on the one hand startling since to our best knowledge they have never been reported in benzimidazole treatment systems. On the other hand, it has been proposed that induced mitotic catastrophe might act as a prestage to apoptosis or necrosis **(58)**, which could be this case. Since we had no further data we cannot confirm this possibility although several morphological indices seem support it and further inquiry into this phenomenon might be needed.

9. CONCLUSION

Our research was focused on investigation of biological activities and in particular antiproliferative potential of benzimidazole carbamate derivative FLU in the *in vitro* model human skin melanoma. Concerning our original aims we have reached the following conclusions:

1. In the human malignant melanoma cell lines of differing molecular profile (A-375, BOWES and RPMI-7951) FLU shows time and concentration dependent cytotoxity during up to 72 hours of exposure. The FLU cytotoxity varies among individual treated cells and is reflected with particular determined IC_{50} values (A375 - IC_{50} = 0.96 µM, BOWES - IC_{50} = 0.90 µM and RPMI-7951 - IC_{50} = 0.25 µM).

2. FLU concentration of 1 µM as chosen for further testing has a cytostatic rather than cytotoxic effect in normal human skin melanocytes. In these cells FLU induces morphological changes, slows proliferation and causes limited activation of cell death. The observed effects are time-limited, however, and at the end of the testing time period they start to abate. It is thus concluded that FLU exposure is at least in melanocytes tolerated.

3. 1 µM FLU induces in exposed melanoma cell lines G2/M phase block, increases the expression of cell cycle inhibitor p21 and produces a series of morphological changes including formation of giant multinucleated cells as well as vacuolated cells. FLU interacts with microtubules of both dividing and interphase cells and is responsible for starting the process of mitotic catastrophe. FLU-simulated mitotic catastrophe leads to apoptosis in exposed melanoma cells characterized by increased activities of caspase-2 and -3/7 and typical nuclear and membrane morphologies. Neither TP53 nor BAX or BCL-2 proteins are directly and universally involved in FLU-dependent apoptosis and thus further inquiries into this mechanism are needed.

4. Explant cultures of five human excised melanomas of differing histopathological grade were established to allow for their FLU-sensitivity testing. Due to their heterogeneity and varying biological properties only cells derived from one sample were used for pilot testing. Their sensitivity to FLU proved to be lower than in stabilized melanoma cell lines (IC_{50} = 1.42 µM). When exposed to sub IC_{50} dose of 1 µM FLU melanoma cells slow their growth and display a series of distinct morphological changes dissimilar to the ones observed in stabilized melanoma lines. Their death morphology is also different.

10. REFERENCES

1. GARBE, Claus, PERIS, Ketty, HAUSCHILD, Axel, SAIAG, Philippe, MIDDLETON, Mark, BASTHOLT, Lars, GROB, Jean-Jacques, MALVEHY, Josep, NEWTON-BISHOP, Julia, STRATIGOS, Alexander J., PEHAMBERGER, Hubert and EGGERMONT, Alexander M., 2016. Diagnosis and treatment of melanoma. European consensus-based interdisciplinary guideline – Update 2016. *European Journal of Cancer*. 1 August 2016. Vol. 63, p. 201–217.
2. LEITER, U. and GARBE, C., 2008. Epidemiology of Melanoma and Nonmelanoma Skin Cancer-The Role of Sunlight. In: [online]. Springer, New York, NY. p. 89–103. Advances in Experimental Medicine and Biology. ISBN 9780387775739.
3. GARBE, Claus and LEITER, Ulrike, 2009. Melanoma epidemiology and trends. *Clinics in Dermatology*. 1 January 2009. Vol. 27, no. 1, p. 3–9.
4. VIERA BAJČIOVÁ, 2016. Maligní melanom a nové možnosti jeho léčby. 2016. Vol. 10, no. 6, p. 256–262.
5. LAKOMÝ RADEK, 2013. Současné možnosti léčby pokročilého a metastatického maligního melanomu. *ONKOLOGIE*. 2013. Vol. 7, no. 2, p. 65–68.
6. HOUGHTON, Alan N. and POLSKY, David, 2002. Focus on melanoma. *Cancer Cell*. 1 October 2002. Vol. 2, no. 4, p. 275–278.
7. TSAO, Hensin, ATKINS, Michael B. and SOBER, Arthur J., 2004. Management of Cutaneous Melanoma. *New England Journal of Medicine*. 2 September 2004. Vol. 351, no. 10, p. 998–1012.
8. GILCHREST, Barbara A., ELLER, Mark S., GELLER, Alan C. and YAAR, Mina, 1999. The Pathogenesis of Melanoma Induced by Ultraviolet Radiation. *New England Journal of Medicine*. 29 April 1999. Vol. 340, no. 17, p. 1341–1348.
9. GRAY-SCHOPFER, Vanessa, WELLBROCK, Claudia and MARAIS, Richard, 2007. Melanoma biology and new targeted therapy. *Nature*. 22 February 2007. Vol. 445, no. 7130, p. 851–857.

10. Types of Melanoma. [online]. [Accessed 14 September 2017]. Available from: http://courses.washington.edu/hubio567/melanoma/types.htm
11. ABCDEs of Melanoma, 2013. *Melanoma Research Foundation* [online]. [Accessed 15 September 2017]. Available from: https://www.melanoma.org/understand-melanoma/diagnosing-melanoma/detection-screening/abcdes-melanoma
12. SOBIN, L. H., 2001. TNM: principles, history, and relation to other prognostic factors. *Cancer*. 15 April 2001. Vol. 91, no. 8 Suppl, p. 1589–1592.
13. Melanoma Skin Cancer Stages, [no date]. [online]. [Accessed 17 September 2017]. Available from: https://www.cancer.org/cancer/melanoma-skin-cancer/detection-diagnosis-staging/melanoma-skin-cancer-stages.html
14. BRESLOW, A, 1970. Thickness, cross-sectional areas and depth of invasion in the prognosis of cutaneous melanoma. *Annals of Surgery*. November 1970. Vol. 172, no. 5, p. 902–908.
15. CLARK, W. H., ELDER, D. E., GUERRY, D., EPSTEIN, M. N., GREENE, M. H. and VAN HORN, M., 1984. A study of tumor progression: the precursor lesions of superficial spreading and nodular melanoma. *Human Pathology*. December 1984. Vol. 15, no. 12, p. 1147–1165.
16. GEOFFREY A. CHARTERS, 2007. Human metastatic melanoma in vitro. *Melanocyte biology*. 2007. The University of Auckland, New Zeland. [online]. [Accessed 17 September 2017]. Available from: https://www.scribd.com/document/124442315/Melanocyte-Biology
17. SLOMINSKI, Andrzej, TOBIN, Desmond J., SHIBAHARA, Shigeki and WORTSMAN, Jacobo, 2004. Melanin Pigmentation in Mammalian Skin and Its Hormonal Regulation. *Physiological Reviews*. 1 October 2004. Vol. 84, no. 4, p. 1155–1228.
18. CICHOREK, Mirosława, WACHULSKA, Małgorzata, STASIEWICZ, Aneta and TYMIŃSKA, Agata, 2013. Skin melanocytes: biology and development. *Advances in Dermatology and Allergology/Postępy Dermatologii I Alergologii*. February 2013. Vol. 30, no. 1, p. 30–41.
19. PILLAIYAR, Thanigaimalai, MANICKAM, Manoj and JUNG, Sang-Hun, 2017. Recent development of signaling pathways inhibitors of melanogenesis. *Cellular Signalling*. December 2017. Vol. 40, p. 99–115.

20. WASMEIER, Christina, HUME, Alistair N., BOLASCO, Giulia and SEABRA, Miguel C., 2008. Melanosomes at a glance. *J Cell Sci*. 15 December 2008. Vol. 121, no. 24, p. 3995–3999.
21. YAMAGUCHI, Yuji, BRENNER, Michaela and HEARING, Vincent J., 2007. The Regulation of Skin Pigmentation. *Journal of Biological Chemistry*. 21 September 2007. Vol. 282, no. 38, p. 27557–27561.
22. ABDEL-MALEK, Zalfa A., KADEKARO, Ana Luisa and SWOPE, Viki B., 2010. Stepping up melanocytes to the challenge of UV exposure. *Pigment Cell & Melanoma Research*. 1 April 2010. Vol. 23, no. 2, p. 171–186.
23. DAMSKY, W. E. and BOSENBERG, M., 2017. Melanocytic nevi and melanoma: unraveling a complex relationship. *Oncogene*. 19 October 2017. Vol. 36, no. 42, p. 5771–5792.
24. BENNETT, Dorothy C., 2003. Human melanocyte senescence and melanoma susceptibility genes. *Oncogene*. 19 May 2003. Vol. 22, no. 20, p. 3063–3069.
25. HAYWARD, N., 2000. New developments in melanoma genetics. *Current Oncology Reports*. July 2000. Vol. 2, no. 4, p. 300–306.
26. LAWRENCE, Michael S., STOJANOV, Petar, et al., 2013. Mutational heterogeneity in cancer and the search for new cancer-associated genes. *Nature*. 11 July 2013. Vol. 499, no. 7457, p. 214–218.
27. CANCER GENOME ATLAS NETWORK, 2015. Genomic Classification of Cutaneous Melanoma. *Cell*. 18 June 2015. Vol. 161, no. 7, p. 1681–1696.
28. TSAO, Hensin, CHIN, Lynda, GARRAWAY, Levi A. and FISHER, David E., 2012. Melanoma: from mutations to medicine. *Genes & Development*. 1 June 2012. Vol. 26, no. 11, p. 1131–1155.
29. MARTINEZ-CARDÚS, Anna, VIZOSO, Miguel, MORAN, Sebastian and MANZANO, Jose Luis, 2015. Epigenetic mechanisms involved in melanoma pathogenesis and chemoresistance. *Annals of Translational Medicine*. September 2015. Vol. 3, no. 15, p. 209.
30. SHAIN, A. Hunter, YEH, Iwei, KOVALYSHYN, Ivanka, SRIHARAN, Aravindhan, TALEVICH, Eric, GAGNON, Alexander, DUMMER, Reinhard, NORTH, Jeffrey, PINCUS, Laura, RUBEN, Beth, RICKABY, William, D'ARRIGO, Corrado, ROBSON, Alistair and BASTIAN, Boris C., 2015. The Genetic Evolution of Melanoma from Precursor Lesions. *New England Journal of Medicine*. 12 November 2015. Vol. 373, no. 20, p. 1926–1936.

31. LIN, William M. and FISHER, David E., 2017. Signaling and Immune Regulation in Melanoma Development and Responses to Therapy. *Annual Review of Pathology*. 24 January 2017. Vol. 12, p. 75–102.
32. PALUNCIC, Jasmina, KOVACEVIC, Zaklina, JANSSON, Patric J., KALINOWSKI, Danuta, MERLOT, Angelika M., HUANG, Michael L.-H., LOK, Hiu Chuen, SAHNI, Sumit, LANE, Darius J. R. and RICHARDSON, Des R., 2016. Roads to melanoma: Key pathways and emerging players in melanoma progression and oncogenic signaling. *Biochimica Et Biophysica Acta*. April 2016. Vol. 1863, no. 4, p. 770–784.
33. MOZŪRAITIENĖ, Julija, BIELSKIENĖ, Kristina, ATKOČIUS, Vydmantas and LABEIKYTĖ, Danutė, 2015. Molecular alterations in signal pathways of melanoma and new personalized treatment strategies: Targeting of Notch. *Medicina (Kaunas, Lithuania)*. 2015. Vol. 51, no. 3, p. 133–145.
34. HENNESSY, Bryan T., SMITH, Debra L., RAM, Prahlad T., LU, Yiling and MILLS, Gordon B., 2005. Exploiting the PI3K/AKT pathway for cancer drug discovery. *Nature Reviews. Drug Discovery*. December 2005. Vol. 4, no. 12, p. 988–1004.
35. DAVIES, M A, STEMKE-HALE, K and TELLEZ, C, 2008. A novel AKT3 mutation in melanoma tumours and cell lines. *British Journal of Cancer*. 21 October 2008. Vol. 99, no. 8, p. 1265–1268.
36. BERTOLOTTO, Corine, 2013. Melanoma: From Melanocyte to Genetic Alterations and Clinical Options. *Scientifica* [online]. 2013. Vol. 2013.
37. PALMIERI, Giuseppe, COLOMBINO, Maria, SINI, Maria Cristina, ASCIERTO, Paolo Antonio, LISSIA, Amelia and COSSU, Antonio, 2013. Targeted Therapies in Melanoma: Successes and Pitfalls. [online]. 2013. [Accessed 26 September 2017]. Available from: http://www.intechopen.com/books/melanoma-from-early-detection-to-treatment/targeted-therapies-in-melanoma-successes-and-pitfalls
38. SOENGAS, María S. and LOWE, Scott W., 2003. Apoptosis and melanoma chemoresistance. *Oncogene*. 19 May 2003. Vol. 22, no. 20, p. 3138–3151.
39. CORAZZARI, Marco, FIMIA, Gian Maria, LOVAT, Penny and PIACENTINI, Mauro, 2013. Why is autophagy important for melanoma? Molecular mechanisms and therapeutic implications. *Seminars in Cancer Biology*. October 2013. Vol. 23, no. 5, p. 337–343.

40. Radiation Therapy for Melanoma Skin Cancer, [online]. [Accessed 1 October 2017]. Available from: https://www.cancer.org/cancer/melanoma-skin-cancer/treating/radiation-therapy.html
41. GARBE, Claus, EIGENTLER, Thomas K. and KEILHOLZ, Ulrich, 2011. Systematic Review of Medical Treatment in Melanoma: Current Status and Future Prospects. *The Oncologist*. 1 January 2011. Vol. 16, no. 1, p. 5–24. DOI 10.1634/theoncologist.2010-0190.
42. BERTOLOTTO, Corine, 2013. Melanoma: From Melanocyte to Genetic Alterations and Clinical Options. *Scientifica* [online]. 2013. Vol. 2013. Available from: https://www.ncbi.nlm.nih.gov/pmc/articles/PMC3874946/
43. POL, Jonathan, KROEMER, Guido and GALLUZZI, Lorenzo, 2016. First oncolytic virus approved for melanoma immunotherapy. *OncoImmunology*. 2 January 2016. Vol. 5, no. 1, p. e1115641.
44. LIU, Qi, DAS, Manisit, LIU, Yun and HUANG, Leaf. Targeted Drug Delivery to Melanoma. *Advanced Drug Delivery Reviews* [online]. Available from: http://www.sciencedirect.com/science/article/pii/S0169409X17301977
45. SHIM, Joong Sup and LIU, Jun O., 2014. Recent Advances in Drug Repositioning for the Discovery of New Anticancer Drugs. *International Journal of Biological Sciences*. 2014. Vol. 10, no. 7, p. 654–663.
46. ČÁŇOVÁ, Kristýna, ROZKYDALOVÁ, Lucie and RUDOLF, Emil, 2017. Anthelmintic Flubendazole and Its Potential Use in Anticancer Therapy. *Acta Medica (Hradec Kralove)*. 2017. Vol. 60, no. 1, p. 5–11.
47. LI, Yvonne Y and JONES, Steven JM, 2012. Drug repositioning for personalized medicine. *Genome Medicine*. 30 March 2012. Vol. 4, no. 3, p. 27.
48. YADAV, Geeta and GANGULY, Swastika, 2015. Structure activity relationship (SAR) study of benzimidazole scaffold for different biological activities: A mini-review. *European Journal of Medicinal Chemistry*. 5 June 2015. Vol. 97, p. 419–443.
49. LACEY, E., 1990. Mode of action of benzimidazoles. *Parasitology Today (Personal Ed.)*. April 1990. Vol. 6, no. 4, p. 112–115.
50. IRELAND, C. M., GULL, K., GUTTERIDGE, W. E. and POGSON, C. I., 1979. The interaction of benzimidazole carbamates with mammalian microtobule

protein. *Biochemical Pharmacology*. 1 September 1979. Vol. 28, no. 17, p. 2680–2682.

51. COOPER, Geoffrey M., 2000. Microtubules. [online]. 2000. [Accessed 20 July 2016]. Available from: http://www.ncbi.nlm.nih.gov/books/NBK9932/
52. JORDAN, Mary Ann and WILSON, Leslie, 2004. Microtubules as a target for anticancer drugs. *Nature Reviews Cancer*. April 2004. Vol. 4, no. 4, p. 253–265.
53. JASRA, N., SANYAL, S. N. and KHERA, S., 1990. Effect of thiabendazole and fenbendazole on glucose uptake and carbohydrate metabolism in Trichuris globulosa. *Veterinary Parasitology*. March 1990. Vol. 35, no. 3, p. 201–209.
54. CUMINO, Andrea C., ELISSONDO, María Celina and DENEGRI, Guillermo M., 2009. Flubendazole interferes with a wide spectrum of cell homeostatic mechanisms in Echinococcus granulosus protoscoleces. *Parasitology International*. September 2009. Vol. 58, no. 3, p. 270–277.
55. ZHANG, Lan, GUO, Mingrui, et al., 2015. Systems biology-based discovery of a potential Atg4B agonist (Flubendazole) that induces autophagy in breast cancer. *Molecular BioSystems*. 13 October 2015. Vol. 11, no. 11, p. 2860–2866.
56. KRÁLOVÁ, Věra, HANUŠOVÁ, Veronika, RUDOLF, Emil, ČÁŇOVÁ, Kristýna and SKÁLOVÁ, Lenka, 2016. Flubendazole induces mitotic catastrophe and senescence in colon cancer cells in vitro. *Journal of Pharmacy and Pharmacology*. 1 February 2016. Vol. 68, no. 2, p. 208–218.
57. KRÁLOVÁ, Věra, HANUŠOVÁ, Veronika, STAŇKOVÁ, Petra, KNOPPOVÁ, Kateřina, ČÁŇOVÁ, Kristýna and SKÁLOVÁ, Lenka, 2013. Antiproliferative effect of benzimidazole anthelmintics albendazole, ricobendazole, and flubendazole in intestinal cancer cell lines. *Anti-Cancer Drugs*. October 2013. Vol. 24, no. 9, p. 911–919.
58. VAKIFAHMETOGLU, H., OLSSON, M. and ZHIVOTOVSKY, B., 2008. Death through a tragedy: mitotic catastrophe. *Cell Death and Differentiation*. July 2008. Vol. 15, no. 7, p. 1153–1162.
59. CASTEDO, Maria, PERFETTINI, Jean-Luc, ROUMIER, Thomas, VALENT, Alexander and RASLOVA, Hana, 2004. Mitotic catastrophe constitutes a special case of apoptosis whose suppression entails aneuploidy. *Oncogene*. May 2004. Vol. 23, no. 25, p. 4362–4370.

60. RONINSON, Igor B., BROUDE, Eugenia V. and CHANG, Bey-Dih, 2001. If not apoptosis, then what? Treatment-induced senescence and mitotic catastrophe in tumor cells. *Drug Resistance Updates*. 1 October 2001. Vol. 4, no. 5, p. 303–313.
61. SOROKINA, Irina V., DENISENKO, Tatiana V., IMREH, Gabriela, TYURIN-KUZMIN, Pyotr A., KAMINSKYY, Vitaliy O., GOGVADZE, Vladimir and ZHIVOTOVSKY, Boris, 2017. Involvement of autophagy in the outcome of mitotic catastrophe. *Scientific Reports*. 6 November 2017. Vol. 7, no. 1, p. 14571.
62. MANSILLA, Sylvia, PRIEBE, Waldemar and PORTUGAL, José, 2006. Mitotic Catastrophe Results in Cell Death by Caspase-Dependentand Caspase-Independent Mechanisms. *Cell Cycle*. 1 January 2006. Vol. 5, no. 1, p. 53–60.
63. GORDON, David J., RESIO, Benjamin and PELLMAN, David, 2012. Causes and consequences of aneuploidy in cancer. *Nature Reviews Genetics*. March 2012. Vol. 13, no. 3, p. 189–203.
64. ESCANDON, J., KING, L., BLOBSTEIN, R., ELLER, M. S. and AURICH-COSTA, J., 2016. Aneuploidy and Tetraploidy as Distinct Patterns During Melanomagenesis. *Surgical technology international*. October 2016. Vol. XXIX, p. 53–59.
65. JANSSEN, Aniek, KOPS, Geert J. P. L. and MEDEMA, René H., 2009. Elevating the frequency of chromosome mis-segregation as a strategy to kill tumor cells. *Proceedings of the National Academy of Sciences*. 10 November 2009. Vol. 106, no. 45, p. 19108–19113.
66. POURGHOLAMI, M. H, WOON, L and ALMAJD, R, 2001. In vitro and in vivo suppression of growth of hepatocellular carcinoma cells by albendazole. *Cancer Letters*. 10 April 2001. Vol. 165, no. 1, p. 43–49.
67. WARENIUS, H. M., JONES, M., GORMAN, T. and MCLEISH, R., 2000. Combined RAF1 protein expression and p53 mutational status provides a strong predictor of cellular radiosensitivity. *British Journal of Cancer*. October 2000. Vol. 83, no. 8, p. 1084–1095.
68. VALIRON, O., CAUDRON, N. and JOB, D., 2001. Microtubule dynamics. *Cellular and molecular life sciences: CMLS*. December 2001. Vol. 58, no. 14, p. 2069–2084.

69. FOJO, Antonio Tito and ADELBERG, David E., 2010. Microtubule Targeting Agents. In: *Drug Management of Prostate Cancer* [online]. Springer, New York, NY. p. 179–194. [Accessed 22 January 2018]. ISBN 978-1-60327-831-7.
70. ZHOU, Jun and GIANNAKAKOU, Paraskevi, 2005. Targeting microtubules for cancer chemotherapy. *Current Medicinal Chemistry. Anti-Cancer Agents*. January 2005. Vol. 5, no. 1, p. 65–71.
71. KHALILZADEH A, WANGOO KT, MORRIS DL, POURGHOLAMI MH. Epothilone-paclitaxel resistant leukemic cells CEM/dEpoB300 are sensitive to albendazole: Involvement of apoptotic pathways. Biochemical Pharmacology 2007 Aug 1; 74(3): 407–14.
72. DOUDICAN, Nicole, RODRIGUEZ, Adrianna, OSMAN, Iman and ORLOW, Seth J., 2008. Mebendazole Induces Apoptosis via Bcl-2 Inactivation in Chemoresistant Melanoma Cells. *Molecular Cancer Research*. 1 August 2008. Vol. 6, no. 8, p. 1308–1315.
73. NYGREN, Peter, FRYKNÄS, Mårten, ÅGERUP, Bengt and LARSSON, Rolf, 2013. Repositioning of the anthelmintic drug mebendazole for the treatment for colon cancer. *Journal of Cancer Research and Clinical Oncology*. 1 December 2013. Vol. 139, no. 12, p. 2133–2140.
74. SASAKI, Ji-ichiro, RAMESH, Rajagopal, CHADA, Sunil, GOMYO, Yoshihito, ROTH, Jack A. and MUKHOPADHYAY, Tapas, 2002. The Anthelmintic Drug Mebendazole Induces Mitotic Arrest and Apoptosis by Depolymerizing Tubulin in Non-Small Cell Lung Cancer Cells. *Molecular Cancer Therapeutics*. 1 November 2002. Vol. 1, no. 13, p. 1201–1209.
75. SPAGNUOLO, Paul A., HU, Jiayi, HURREN, Rose, WANG, Xiaoming and GRONDA, Marcela, 2010. The antihelmintic flubendazole inhibits microtubule function through a mechanism distinct from Vinca alkaloids and displays preclinical activity in leukemia and myeloma. *Blood*. 10 June 2010. Vol. 115, no. 23, p. 4824–4833.
76. HOU, Zhi-Jie, LUO, Xi, ZHANG, Wei, et al., 2015. Flubendazole, FDA-approved anthelmintic, targets breast cancer stem-like cells. *Oncotarget*. 27 February 2015. Vol. 6, no. 8, p. 6326–6340.
77. MICHAELIS, Martin, AGHA, Bishr and ROTHWEILER, Florian, 2015. Identification of flubendazole as potential anti-neuroblastoma compound in a large cell line screen. *Scientific Reports*. 3 February 2015. Vol. 5.

78. MITCHISON, Tim and KIRSCHNER, Marc, 1984. Dynamic instability of microtubule growth. *Nature*. November 1984. Vol. 312, no. 5991, p. 237–242.
79. CASTEDO, Maria, PERFETTINI, Jean-Luc, ROUMIER, Thomas, ANDREAU, Karine, MEDEMA, Rene and KROEMER, Guido, 2004. Cell death by mitotic catastrophe: a molecular definition. *Oncogene*. April 2004. Vol. 23, no. 16, p. 2825–2837.
80. MORRIS, V. B., BRAMMALL, J., NOBLE, J. and REDDEL, R., 2000. p53 localizes to the centrosomes and spindles of mitotic cells in the embryonic chick epiblast, human cell lines, and a human primary culture: An immunofluorescence study. *Experimental Cell Research*. 10 April 2000. Vol. 256, no. 1, p. 122–130.
81. ČÁŇOVÁ, K., ROZKYDALOVÁ, L., VOKURKOVÁ, D. and RUDOLF, E., 2018. Flubendazole induces mitotic catastrophe and apoptosis in melanoma cells. *Toxicology in vitro: an international journal published in association with BIBRA*. February 2018. Vol. 46, p. 313–322.
82. DAWAR, S., LIM, Y., PUCCINI, J., WHITE, M., THOMAS, P., BOUCHIER-HAYES, L., GREEN, D. R., DORSTYN, L. and KUMAR, S., 2017. Caspase-2-mediated cell death is required for deleting aneuploid cells. *Oncogene*. May 2017. Vol. 36, no. 19, p. 2704–2714.
83. TERRANO, David T., UPRETI, Meenakshi and CHAMBERS, Timothy C., 2010. Cyclin-dependent kinase 1-mediated Bcl-xL/Bcl-2 phosphorylation acts as a functional link coupling mitotic arrest and apoptosis. *Molecular and Cellular Biology*. February 2010. Vol. 30, no. 3, p. 640–656.
84. HARLEY, Margaret E., ALLAN, Lindsey A., SANDERSON, Helen S. and CLARKE, Paul R., 2010. Phosphorylation of Mcl-1 by CDK1-cyclin B1 initiates its Cdc20-dependent destruction during mitotic arrest. *The EMBO journal*. 21 July 2010. Vol. 29, no. 14, p. 2407–2420.
85. SHI, Jue, ZHOU, Yuan, HUANG, Hsiao-Chun and MITCHISON, Timothy J., 2011. Navitoclax (ABT-263) accelerates apoptosis during drug-induced mitotic arrest by antagonizing Bcl-xL. *Cancer Research*. 1 July 2011. Vol. 71, no. 13, p. 4518–4526.
86. TUNQUIST, Brian J., WOESSNER, Richard D. and WALKER, Duncan H., 2010. Mcl-1 stability determines mitotic cell fate of human multiple myeloma

tumor cells treated with the kinesin spindle protein inhibitor ARRY-520. *Molecular Cancer Therapeutics*. July 2010. Vol. 9, no. 7, p. 2046–2056.

87. SAKURIKAR, Nandini, EICHHORN, Joshua M., ALFORD, Sarah E. and CHAMBERS, Timothy C., 2014. Identification of a mitotic death signature in cancer cell lines. *Cancer Letters*. 28 February 2014. Vol. 343, no. 2, p. 232–238.
88. MC GEE, Margaret M., 2015. Targeting the Mitotic Catastrophe Signaling Pathway in Cancer. *Mediators of Inflammation*. 2015. Vol. 2015, p. 146282.
89. DOUDICAN, Nicole A., BYRON, Sara A., POLLOCK, Pamela M. and ORLOW, Seth J., 2013. XIAP downregulation accompanies mebendazole growth inhibition in melanoma xenografts. *Anti-Cancer Drugs*. February 2013. Vol. 24, no. 2, p. 181–188.